Electronic Supplementary Material (ESI) for Journal of Materials Chemistry A.
This journal is © The Royal Society of Chemistry 2022

Polystyrene-supported neutral lithium receptor for the recovery of high-purity $LiPF_6$ from simulated degraded electrolyte

Sheng-Yin Huang, Hu Wang, Hugo Celio, Niveen M. Khashab, Zachariah A. Page, Jonathan L. Sessler

Supporting Information

Table of Contents

Synthesis 5

Scheme S1. Synthesis of L 6

Scheme S2. Synthetic Scheme of P3. 7

ATR-IR spectra 8

Figure S1. ATR-IR spectra of monomer 4 and P2. 8

Figure S2. ATR-IR spectra of $LiPF_6$ and P2•$LiPF_6$. 8

Figure S3. ATR-IR spectra of P2•LiPF6 and regenerated P2. 9

Loading level determination 10

Figure S4. Determination of loading. 10

Figure S5. Time-dependent chemical shift changes. 11

Binding stoichiometry determination 12

Figure S6. Job's plot of of L + $LiPF_6$ in CD_3CN 12

Figure S7. ESI-HRMS spectrum of L•$LiPF_6$. 13

Binding constant determination 14

Figure S8. NMR spectroscopic titration of L with $LiPF_6$ in CD_3CN (blue) and CD_3OD (red). 14

Figure S9. NMR spectroscopic titration of L with $NaPF_6$ (blue) and KPF_6 (red) in CD_3CN. 15

Figure S10. Solid state ^{31}P and ^{7}Li NMR spectra of P2•$LiPF_6$ 16

Figure S11. ^{31}P, ^{19}F, and ^{7}Li NMR spectra of the $LiPF_6$ presumed to be released in MeOH 17

Energy dispersive X-ray analysis of P2•$LiPF_6$ 18

Figure S12. EDX spectrum of P2•$LiPF_6$. 18

Table S1. Elemental analysis of P2•$LiPF_6$ by EDX. 18

Calibration curves for conductivity measurements of $LiPF_6$ concentration 19

Figure S13. Calibration curves of $LiPF_6$ concentration determined by conductivity measurements 19

Quantitative NMR (qNMR) spectral studies 20

Figure S14. FID spectrum of ^{19}F in $LiPF_6$ as recorded in ACN 21

Figure S15. INVREC spectra of $LiPF_6$ in ACN 22

Figure S16. ^{19}F qNMR spectra of (a) degraded and (b) $K_2CO_{3(g)}$ neutralized samples 23

Figure S17. ^{19}F qNMR spectra of $LiPF_6$ in ACN 24

Table S2. ICP-MS result of the recovered product. 24

NMR and MS spectra 25

Figure S18. ^{1}H NMR spectrum of 2-bromo-N,N-dicyclohexylacetamide (400 MHz, $CDCl_3$). 25

Figure S19. ^{13}C NMR spectrum of 2-bromo-N,N-dicyclohexylacetamide (100 MHz, $CDCl_3$). 25
Figure S20. ESI-HRMS spectrum of compound 2-bromo-N,N-dicyclohexylacetamide 26
Figure S21. ^{1}H NMR spectrum of compound 1 (400 MHz, $CDCl_3$). 27
Figure S22. ^{13}C NMR spectrum of compound 1 (100 MHz, $CDCl_3$). 27
Figure S23. ESI-HRMS spectrum of compound 1 28
Figure S24. 1H NMR spectrum of compound 2 (400 MHz, $CDCl_3$) 29
Figure S25. ^{13}C NMR spectrum of compound 2 (100 MHz, $CDCl_3$). 29
Figure S26. ESI-HRMS spectrum of compound 2 30
Figure S27. ^{1}H NMR spectrum of compound 3 (400 MHz, $CDCl_3$). 31
Figure S28. ^{13}C NMR spectrum of compound 3 (100 MHz, $CDCl_3$). 31
Figure S29. ESI-HRMS spectrum of compound 3 32
Figure S30. ^{1}H NMR spectrum of compound 4 (400 MHz, $CDCl_3$) 33
Figure S31. ^{13}C NMR spectrum of compound 4 (100 MHz, $CDCl_3$). 33
Figure S32. ESI-HRMS spectrum of compound 4. 34
Figure S33. ^{1}H NMR spectrum of compound L (400 MHz, $CDCl_3$). 35
Figure S34. ^{13}C NMR spectrum of compound L (100 MHz, $CDCl_3$). 35
Figure S35. ESI-HRMS spectrum of compound L 36
Cost Analyses 37
Figure S36. Cost analysis of crown-ether functionalized polystyrene resin 37
Figure S37. Cost analysis of P2 37
X-Ray Photoelectron Spectroscopic Analyses 38
Figure S38. XPS analyses of P2•$LiPF_6$ (green) and P2 (red). 38
References 39

General considerations. Unless otherwise stated, all chemicals were purchased from commercial suppliers and used without further purification. Deuterated solvents were obtained from Cambridge Isotope Laboratories (Tewskbury, MA, USA). Anhydrous methanol was distilled over KOH. Anhydrous acetonitrile was distilled over CaH. Anhydrous tetrahydrofuran was purchased from ThermoScientific. Aminomethyl polystyrene resin was purchased from ChemImpex. Flash chromatography was performed on Merck silica gel. ^{1}H, ^{13}C, ^{19}F, ^{31}P, and ^{7}Li NMR spectra were recorded at the NMR facility of the Department of Chemistry of The University of Texas at Austin. Unless otherwise specified, the residual solvent peaks were used as the internal references for the NMR spectra analyses. Data for ^{1}H NMR are recorded as follows: chemical shift (δ, ppm), multiplicity (s, singlet; d, doublet, t, triplet; q, quartet; br, broad; m, multiplet), coupling constant (Hz), integration. Data for ^{13}C NMR are recorded as follows: chemical shift (δ, ppm). High resolution electrospray spray ionization time-of-flight mass spectrometry (HR-ESI/TOF-MS) service was provided by the mass spectrometry facility at the department of Chemistry of the University of Texas at Austin. Attenuated total reflectance – infrared (ATR-IR) spectra were recorded on an Infinity Gold FTIR at the Texas Materials Institute of The University of Texas at Austin. Inductively coupled plasma mass spectrometry (ICP-MS) analysis service was provided by the quadrupole ICP-MS lab at Jackson School of Geoscience at The University of Texas at Austin. Elemental analysis service was provided by mass spectrometry facility at the Department of Chemistry & Biochemistry of the Texas Tech University. An Oakton CON 550 replacement conductivity cell K = 0.1 probe was used for the conductivity measurements. Data processing was performed using the QtiPlot 1.0.0.0 software.

Synthesis

2-Bromo-*N*,*N*-dicyclohexylacetamide was prepared according to a reported procedure.[1] The structure was characterized and confirmed by ^{1}H and ^{13}C NMR spectroscopy, as well as ESI-HRMS.

2,5-Dioxopyrrolidin-1-yl methyl glutarate 5-methoxy-5-oxopentanoate (1). Monomethyl glutarate (811 mg, 5.55 mmol), 1-ethyl-3-(3-dimethylaminopropyl)carbodiimide hydrochloride (EDCI) (1.06 g, 5.55 mmol), and *N*-hydroxysuccinimide (639 mg, 5.55 mmol) were dissolved in methylene chloride (50 mL). The solution was stirred at room temperature for 6 h before washing with saturated $NaHCO_{3(aq)}$. The washed organic layer was dried over anhydrous $MgSO_{4(g)}$, filtered, and concentrated under reduced pressure. The residue was purified by flash chromatography over silica gel using 55% ethyl acetate/45% hexanes as the eluent to yield **1** as colorless liquid. (1.21 g, 90%). ^{1}H NMR (400 MHz, $CDCl_3$): δ = 3.63 (s, 3 H), 2.78 (s, 4 H), 2.65 (t, 2H, J = 8 Hz), 2.42 (t, 2H, J = 8 Hz), 2.06-1.96 (m, 2H). ^{13}C NMR (100 MHz, $CDCl_3$): δ = 172.81, 169.25, 168.07, 51.61, 32.30, 29.90, 25.50, 19.68. ESI-HRMS: *m/z* = 266.0643 ($[M+H]^+$), (calcd. 266.0635).

***Tert*-butyl (1,3-bis(2-(dicyclohexylamino)-2-oxoethoxy)propan-2-yl)carbamate-tert-butyl (1,3-dihydroxypropan-2-yl)carbamate-2-bromo-N,N-dicyclohexylacetamide (2).** To a suspension of 60% NaH (188 mg, 4.71 mmol) in anhydrous THF (20 mL) was added BOC-protected serinol (300 mg, 1.57 mmol). After the effervescence stopped, 2-bromo-*N*,*N*-dicyclohexylacetamide (948 mg, 3.14 mmol) dissolved in anhydrous THF (10 mL) was slowly injected into the NaH solution. After allowing to sit for 1 h at room temperature, water was slowly added to the mixture. The volatiles were then removed under vacuum. The residue was then dissolved in CH_2Cl_2, washed with water, dried over $MgSO_{4(g)}$, filtered, and concentrated under reduced pressure. The residue was purified by flash chromatography over silica gel using 40% ethyl acetate/60% hexanes as the eluent to yield **2** as foam-like liquid. (796 mg, 80%). ^{1}H NMR (400 MHz, $CDCl_3$): δ = 4.12-4.02 (m, 4H), 3.83 (br, 1H), 3.71-3.50 (m, 4H), 3.31 (br, 2H), 2.90 (br, 2H), 2.43 (br, 4H), 1.84-1.72 (m, 8H), 1.72-1.61 (m, 6H), 1.56 (br, 2H), 1.52-1.42 (m, 8H), 1.42-1.38 (m, 9H), 1.34-1.02 (m, 13H). ^{13}C NMR (100 MHz, $CDCl_3$): δ = 168.15, 155.75, 79.19, 71.55, 70.18, 57.17, 56.26, 31.35, 29.96, 28.49, 26.68, 26.00, 25.41, 25.33. ESI-HRMS: *m/z* = 634.4790 ($[M+H]^+$), (calcd. 634.4790).

Methyl 5-((1,3-bis(2-(dicyclohexylamino)-2-oxoethoxy)propan-2-yl)amino)-5-oxopentanoate--2,2'-((2-aminopropane-1,3-diyl)bis(oxy))bis(N,N-dicyclohexylacetamide) (3). Compound **2** (753 mg, 1.19 mmol) was first dissolved in CH_2Cl_2 (10 mL) before trifluoroacetic acid (10 mL) was slowly added to the solution. After stirring at room temperature for 2 h, the volatiles were removed under high vacuum. The residue was dissolved in CH_2Cl_2 (10 mL) and neutralized with 1N aqueous NaOH. The organic layer was separated, dried over anhydrous $MgSO_{4(g)}$, filtered, and concentrated under reduced pressure. The residue was redissolved in CH_2Cl_2 (10 mL) and combined with a CH_2Cl_2 (10 mL) solution of the glutarate linker **1** (289 mg, 1.19 mmol) and allowed to react at room temperature for 6 h. After washing with saturated $NaHCO_{3(aq)}$, the organic layer was dried over anhydrous $MgSO_{4(g)}$, filtered, and concentrated under reduced pressure. The residue was purified by flash chromatography over silica gel using 100% ethyl acetate to yield **3** as colorless liquid. (591 mg, 75%). ^{1}H NMR (400 MHz, $CDCl_3$): δ = 8.02 (br, 1H), 4.16-3.99 (m, 5H), 3.76-3.69 (m, 2H), 3.63 (s, 3H), 3.60-3.50 (m, 2H), 3.22 (br, 2H), 2.90 (br, 2H), 2.55-2.31 (m, 6H), 2.31-2.18 (m, 2H), 2.04-1.92 (m, 2H), 1.85-1.71 (m, 8H), 1.71-1.60 (m, 6H), 1.60-1.53 (m, 2H), 1.53-1.38 (m, 8H), 1.34-0.99 (m, 13H). ^{13}C NMR (100 MHz, $CDCl_3$): δ = 173.73,

172.59, 168.31, 70.69, 69.78, 56.77,56.19, 51.54, 49.64, 5.67,33.53, 31.26, 30.00, 26.66, 25.97, 25.44, 25.27, 20.98. ESI-HRMS: *m/z* = 662.4737 ([M+H]$^+$), (calcd. 662.4739).

2,5-Dioxopyrrolidin-1-yl 5-((1,3-bis(2-(dicyclohexylamino)-2-oxoethoxy)propan-2-yl)amino)-5-oxopentanoate (4). Compound **3** (507 mg, 0.766 mmol) was dissolved in MeOH (10 mL) and saponified using 1N NaOH (2.3 mL) at 60 ^{o}C for 3 h. After removing MeOH under vacuum, to the residue was added water (5 mL) and acidified with 1N HCl until a pH = 3 was reached. The aqueous solution was then extracted with CH_2Cl_2 (3 x 10 mL). The organic layers were combined, dried over anhydrous $MgSO_{4(g)}$, filtered, and concentrated under reduced pressure. NHS (88.0 mg, 0.766 mmol), EDCI (147 mg, 0.766 mmol), and the residue were dissolved in CH_2Cl_2 (10 mL). The mixture was stirred at room temperature for 6 h. The mixture was then washed with 0.1 N aqueous HCl (10 mL). The organic layer was separated, dried over anhydrous $MgSO_{4(g)}$, filtered, and concentrated under reduced pressure. The residue was purified by flash chromatography over silica gel using 100% ethyl acetate to yield monomer **4** as foam-like liquid. (542 mg, 95%). ^{1}H NMR (400 MHz, $CDCl_3$): δ = 7.92 (br, 1H), 4.08-3.89 (m, 5H), 3.67-3.57 (m, 2H), 3.53-3.40 (m, 2H), 3.15 (br, 2H), 2.82 (br, 2H), 2.72 (s, 4H), 2.58 (t, 2H, J = 8 Hz), 2.48-2.12 (m, 6H), 2.04-1.93 (m, 2H), 1.77-1.62 (m, 8H), 1.62-1.51 (m, 6H),1.49 (br, 2H), 1.41-1.30 (m, 7H), 1.29-0.86 (m, 13H). ^{13}C NMR (100 MHz, $CDCl_3$): δ = 171.67, 169.13, 168.15, 167.98, 70.61, 69.59, 56.56, 55.88, 49.37, 34.66, 31.00, 30.02, 29.75, 26.40, 25.71, 25.46, 25.22, 25.02, 20.47. ESI-HRMS: *m/z* = 745.4748 ([M+H]$^+$), (calcd. 745.4746).

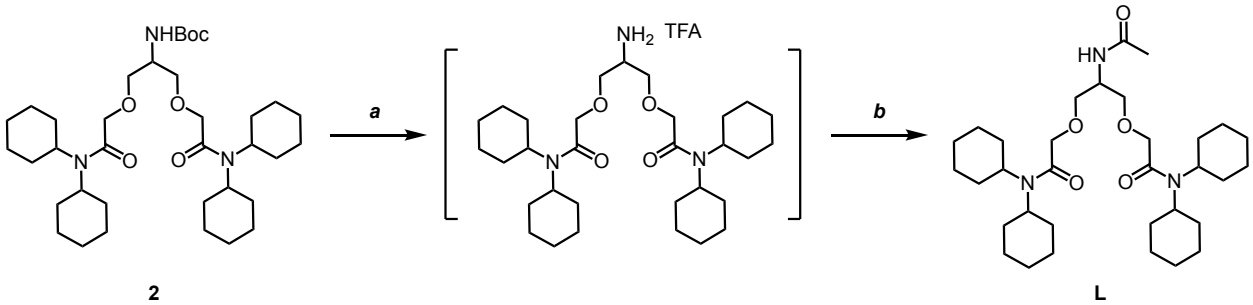

Scheme S1. Synthesis of **L**. Reagents and conditions: (a) CF_3COOH, CH_2Cl_2, rt, 1h; (b) AcOSu, NEt_3, CH_2Cl_2, rt, 6h.

2,2'-((2-Acetamidopropane-1,3-diyl)bis(oxy))bis(N,N-dicyclohexylacetamide) (L). Compound **L** was prepared according to Scheme S1. Compound **2** (300. mg, 0.473 mmol) was first deprotected by stirring with trifluoroacetic acid (5 mL) in CH_2Cl_2 (5 mL) at room temperature for 1 h. The volatiles were then removed under high vacuum. The intermediate TFA salt presumed to be formed in this way was used without further purification. It was first dissolved in CH_2Cl_2 (10 mL), followed by the addition of *N*-acetoxysuccinimide (75 mg, 0.47 mmol) dissolved in CH_2Cl_2 (10 mL). NEt_3 (198 µL, 1.42 mmol) was added to the mixture, and the solution was let stir at room temperature for 6 h. The mixture was then washed with 0.1 N aqueous HCl (10 mL). The organic layer was separated, dried over anhydrous $MgSO_{4(g)}$, filtered, and concentrated under reduced pressure. The residue was purified by flash chromatography over silica gel using 5% MeOH / 95% EtOAc to yield monomer **L** as a foam-like liquid. (205 mg, 75%). ^{1}H NMR (400 MHz, $CDCl_3$): δ = 7.96 (br, 1H), 4.19-3.94 (m, 5H), 3.80-3.67 (m, 2H), 3.66-3.51 (m, 2H), 3.22 (br, 2H), 2.91 (br, 2H), 2.41 (br, 4H), 1.99 (s, 3H), 1.89-1.71 (m, 9H), 1.71-1.58 (m, 7H), 1.56 (br, 2H), 1.51-1.37 (m, 8H), 1.35-1.00 (m, 13H). ^{13}C NMR (100 MHz, $CDCl_3$): δ = 170.65, 168.31, 70.81, 69.89, 56.80, 56.21,

49.73, 31.27, 30.00, 26.66, 25.98, 25.45, 25.27, 23.40. ESI-HRMS: *m/z* = 576.4370 ($[M+H]^+$), (calcd. 576.4371).

P1. Aminomethyl polystyrene resin (1% DVB, 1.6 mmol/g, 100 mg) was first swollen and washed with CH_2Cl_2 (3x10 mL). The resin was resuspended in CH_2Cl_2 (10 mL) in the presence of added monomer **4** (112 mg, 0.150 mmol). The mixture was let stir at room temperature for 6 h. The resin was filtered, rinsed with CH_2Cl_2 until no UV active species was observed on a TLC plate. The resin was then dried under high vacuum to yield **P1**.

P2. *N*-Acetoxysuccinimide (50.3 mg, 0.320 mmol) was added to a suspension of **P1** (100 mg), and the mixture was stirred for 6 h at room temperature. The resin was filtered, rinsed with CH_2Cl_2 until no UV active species was observed on a TLC plate. The resin was then dried under high vacuum to yield **P2**.

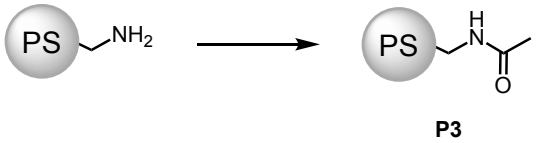

Scheme S2. Synthetic Scheme of **P3**.

P3. The control polymer **P3** was synthesized according to Scheme S2. Aminomethyl polystyrene resin (1% DVB, 1.5 mmol/g, 100 mg) was first swollen and washed with CH_2Cl_2 (3x10 mL). *N*-acetoxysuccinimide (50.3 mg, 0.320 mmol) was added to the suspension of **P3** and the mixture was stirred for 6 h at room temperature. The resin was filtered, rinsed with CH_2Cl_2 until no UV active species was observed on a TLC plate. The resin was then dried under high vacuum to yield **P3**.

ATR-IR spectra

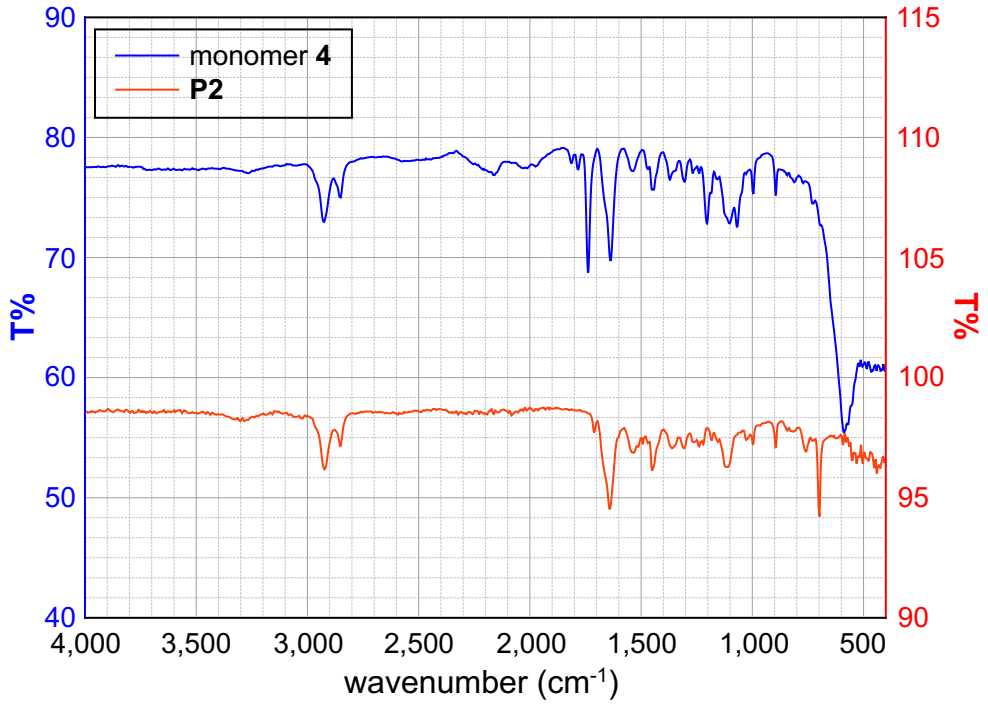

Figure S1. ATR-IR spectra of monomer **4** and **P2**.

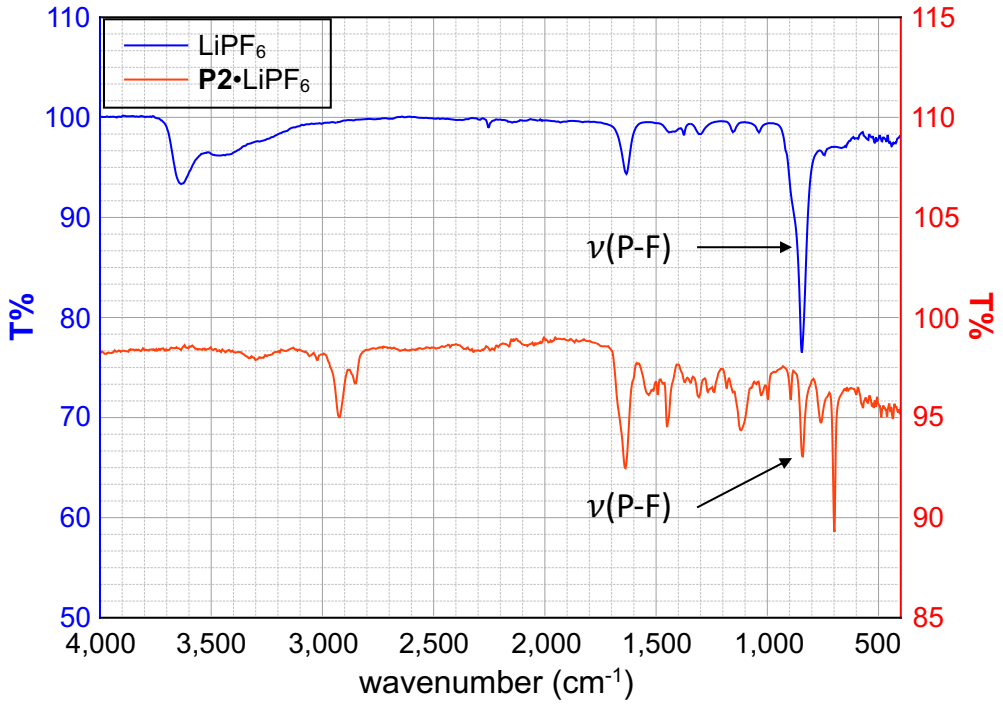

Figure S2. ATR-IR spectra of $LiPF_6$ and **P2**•$LiPF_6$.

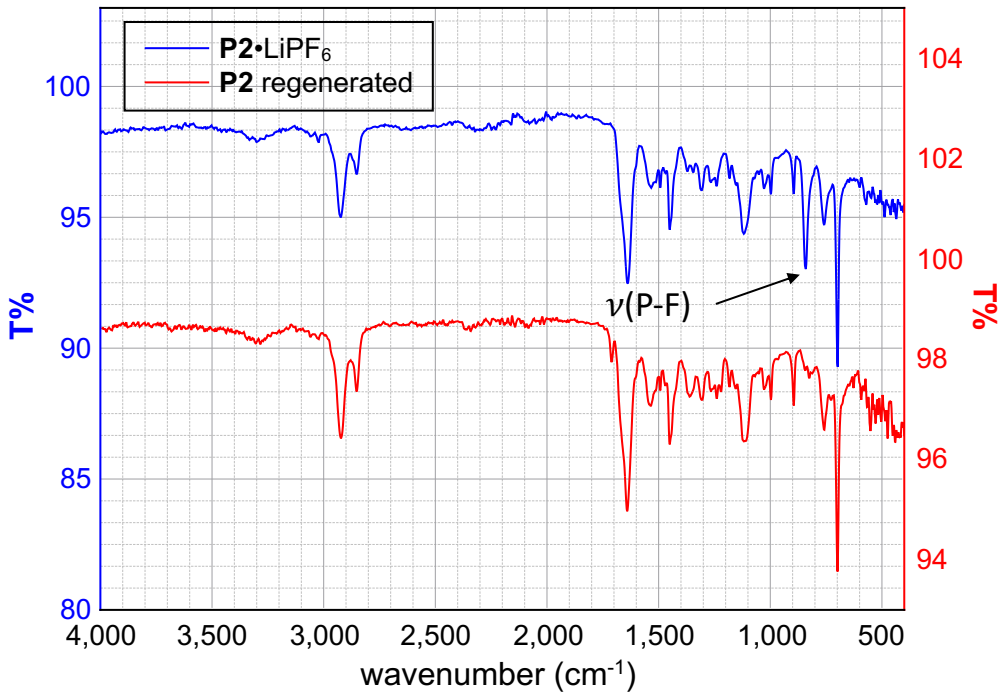

Figure S3. ATR-IR spectra of **P2**•LiPF6 and regenerated **P2**.

Loading level determination

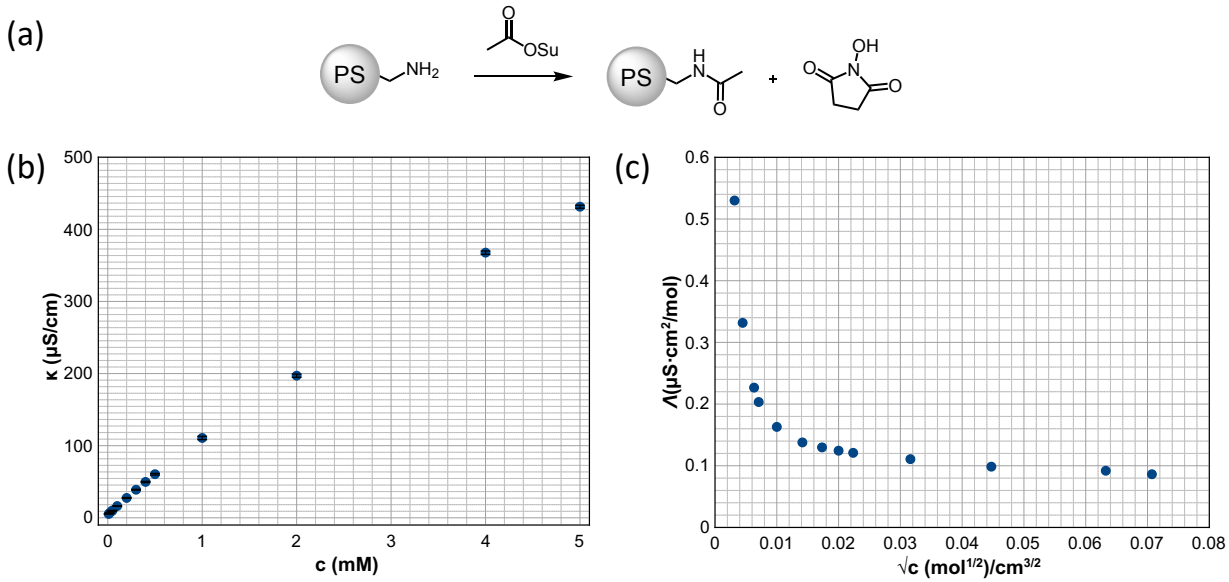

Figure S4. Determination of loading. (a) Reaction scheme. (b) Concentration dependent conductivity of NHS in water. (c) Molar conductivity of NHS in water.

The loading was determined by conductivity measurements involing the eliminated *N*-hydroxysuccinimide (NHS) in water (Figure S4). Since NHS is highly water soluble while both the polymer and *N*-acetoxysuccinimide have negligible water solubility, the conductivity change of the aqueous solution was considered to directly reflect the concentration of the NHS. This method was first verified by comparing the loading of amine provided by the manufacture to that determined using this conductivity protocol. Specifically, this procedure yielded values between 1.42 mmol/g – 1.60 mmol/g, in close agreement with 1.5 mmol/g indicated in the manufacturer's certificate of analysis.

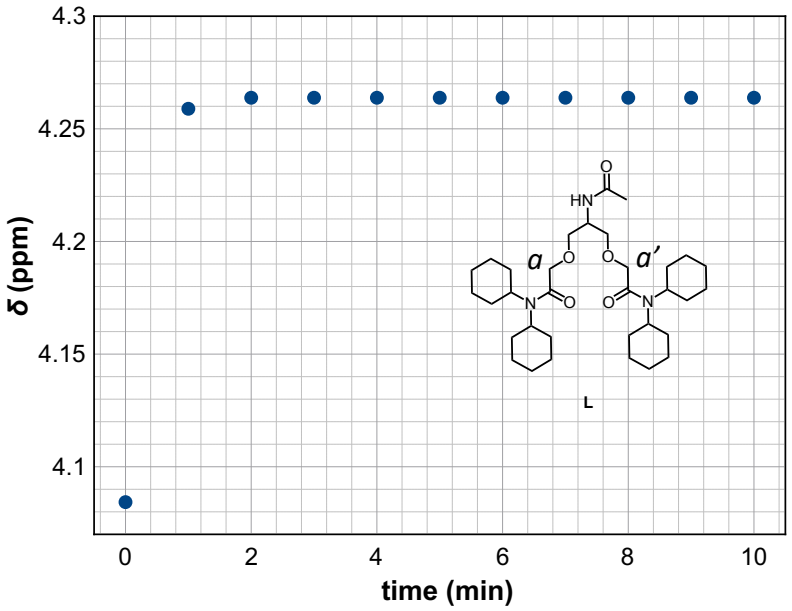

Figure S5. Time-dependent chemical shift changes. Conditions: Conditions: [**L**] = 5 mM, [$LiPF_6$] = 5 mM in CD_3CN. Solutions of $LiPF_6$ were prepared fresh under N_2. δ: chemical shift of protons a or a'.

Binding stoichiometry determination

Job's plot was used to determine the binding stoichiometry of L + $LiPF_6$ and was constructed by NMR spectroscopic studies. A peat at $\boldsymbol{X}_L$ = 0.5 suggests a 1:1 binding ratio (Figure S6).

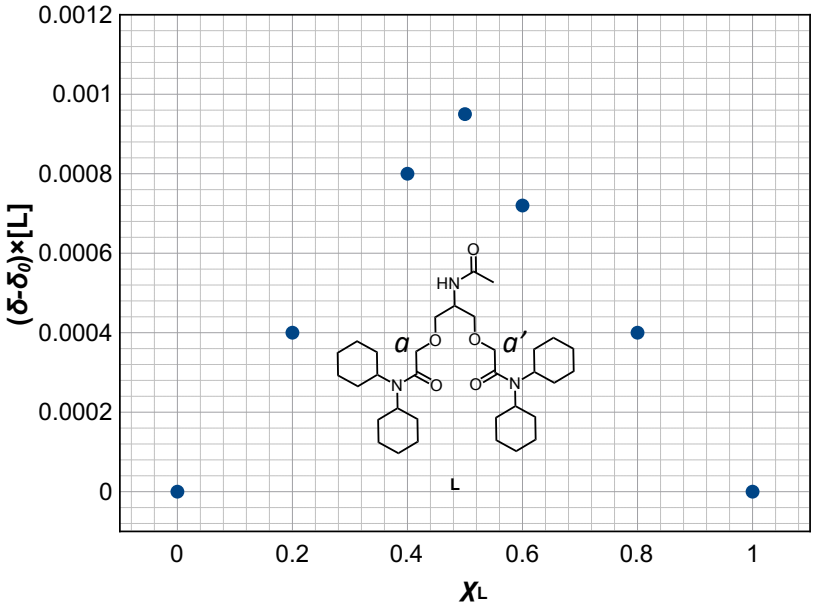

Figure S6. Job's plot of of L + $LiPF_6$ in CD_3CN. Conditions: [L]+[$LiPF_6$] = 10 mM at each molar variation. A time delay of at least 5 min was allowed between measurements to ensure equilibrium is reached (Figure S5). δ: chemical shift of protons a or a'; δ_0: initial chemical shift; $\boldsymbol{X}_L$: [L]/([L]+[$LiPF_6$]).

The 1:1 binding stoichiometry was further supported by the observed isotopic distribution in the ESI-HRMS spectrum of **L**•$LiPF_6$ (Figure S7).

Target Compound Screening Report

Results Acquired by The University of Texas at Austin Mass Spectrometry Facility

Data File	MSF22-0202(Ser-Ac-DCA+LiPF6)_GenthrESIpos3.d	**Sample Name**	0202(Ser-Ac-DCA+LiPF6)	**Comment**	0202(Ser-Ac-DCA+LiPF6)
Position	P1-C3	**Instrument Name**	Instrument 1	**User Name**	
Acq Method	FIA_Gentle.m	**Acquired Time**	2/7/2022 2:44:29 PM	**DA Method**	Amruth.m

MS Zoomed Spectrum

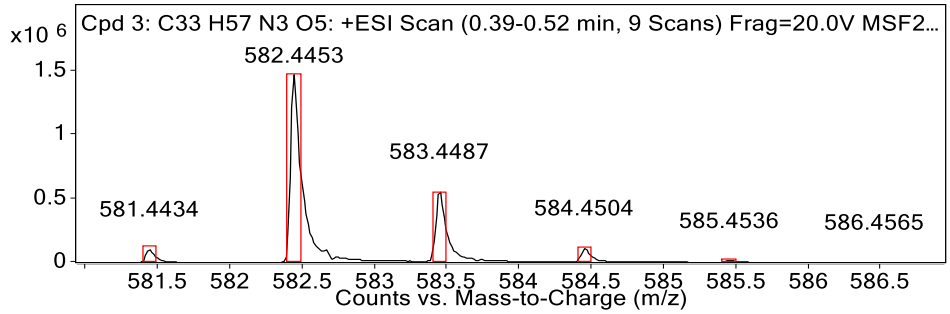

MS Spectrum Peak List

Obs. m/z	Calc. m/z	Charge	Abundance	Formula	Ion Species	Tgt Mass Error (ppm)
581.4434	581.4444	1	104837	C33H57N3O5	(M+Li)+	1.72
582.4453	582.4453	1	1469724	C33H57N3O5	(M+Li)+	0.13
583.4487	583.4485	1	556019	C33H57N3O5	(M+Li)+	-0.27
584.4504	584.4515	1	113942	C33H57N3O5	(M+Li)+	1.75
585.4536	585.4543	1	14739	C33H57N3O5	(M+Li)+	1.13
586.4565	586.4570	1	1747	C33H57N3O5	(M+Li)+	0.79

--- End Of Report ---

Agilent Technologies Page 1 of 1 Printed at: 3:25 PM on:2/7/2022

Figure S7. ESI-HRMS spectrum of **L**•$LiPF_6$.

Binding constant determination

Data fitting of the presumed 1:1 binding equilibrium was made using the following equations:

$$[\mathrm{H}] + [\mathrm{G}] \rightleftharpoons [\mathrm{HG}]$$

where H denotes the host (L), G the guest ($LiPF_6^-$).

Equilibrium constants K are defined as:

$$\mathrm{K} = \frac{[\mathrm{HG}]}{[\mathrm{H}][\mathrm{G}]}$$

The NMR chemical shift change can be described as:

$$\delta = \delta_0 + \delta_{Max}\left(\frac{1}{2[H]_0}\right)\left\{[G]_0 + [H]_0 + \frac{1}{K} - \sqrt{\left([G]_0 + [H]_0 + \frac{1}{K}\right)^2 - 4[H]_0[G]_0}\right\}$$

where

δ: observed chemical shift

δ_0: initial observed chemical shift

δ_{max}: plateaued chemical shift

$[\mathrm{H}]_0$: initial concentration of host

$[\mathrm{G}]_0$: total concentration of guest.

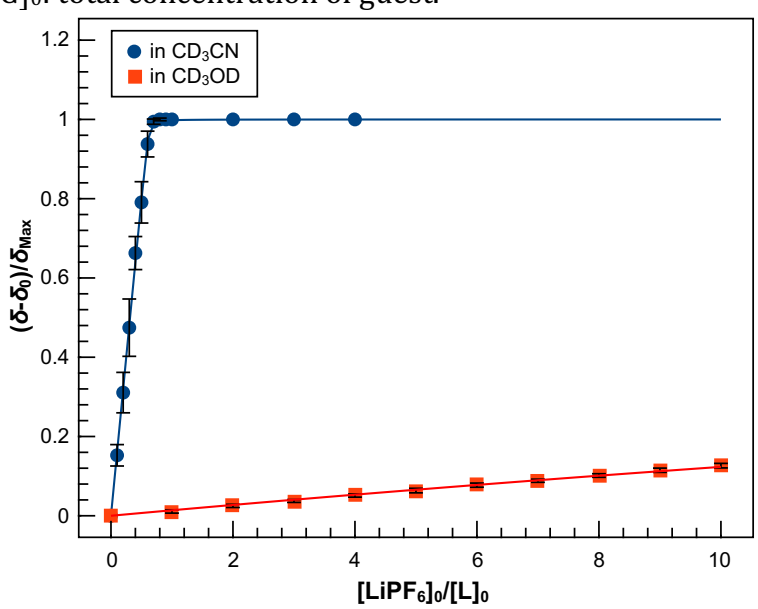

Figure S8. NMR spectroscopic titration of **L** with $LiPF_6$ in CD_3CN (blue) and CD_3OD (red). Conditions: [**L**] = 5 mM. Solutions of $LiPF_6$ were prepared fresh under N_2. A time delay of at least 5 min was allowed between measurements to ensure equilibrium is reached (Figure S5). Error bars represent s.d., *n* =3. δ: chemical shift of protons a or a'; δ_0: initial chemical shift; δ_{Max}: chemical shift when [$LiPF_6$] is saturated.

Fitting results:

$R^2 = 0.9995$

$K = (2.6 \pm 0.2) \times 10^5\ M^{-1}$

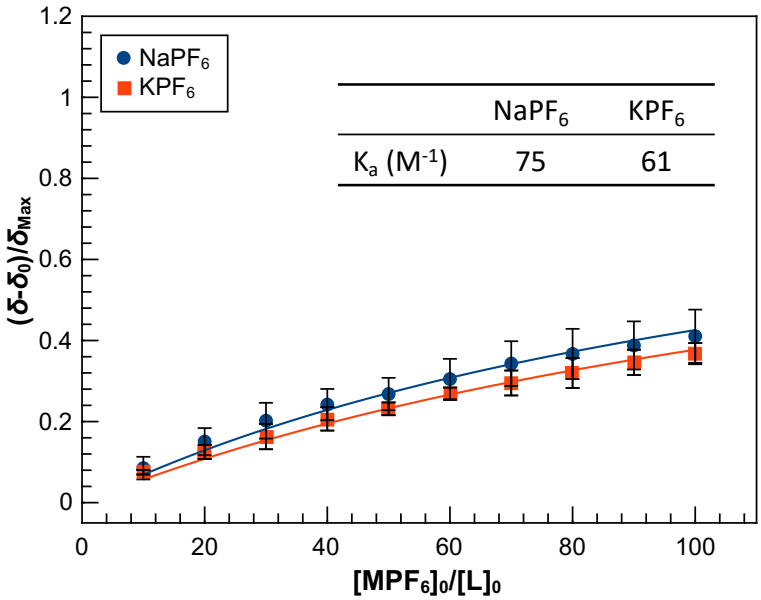

Figure S9. NMR spectroscopic titration of **L** with $NaPF_6$ (blue) and KPF_6 (red) in CD_3CN. Conditions: [**L**] = 0.1 mM. A time delay of at least 5 min was allowed between measurements to ensure equilibrium is reached (Figure S5). Error bars represent s.d., *n* =3. δ: chemical shift of protons a or a'; δ_0: initial chemical shift; δ_{Max}: chemical shift when [$NaPF_6$] or [KPF_6] is saturated.

Fitting results:
[$NaPF_6$]:
R^2= 0.9899
K= 74± 2 M^{-1}

[KPF_6]:
R^2= 0.9926
K= 61± 1 M^{-1}

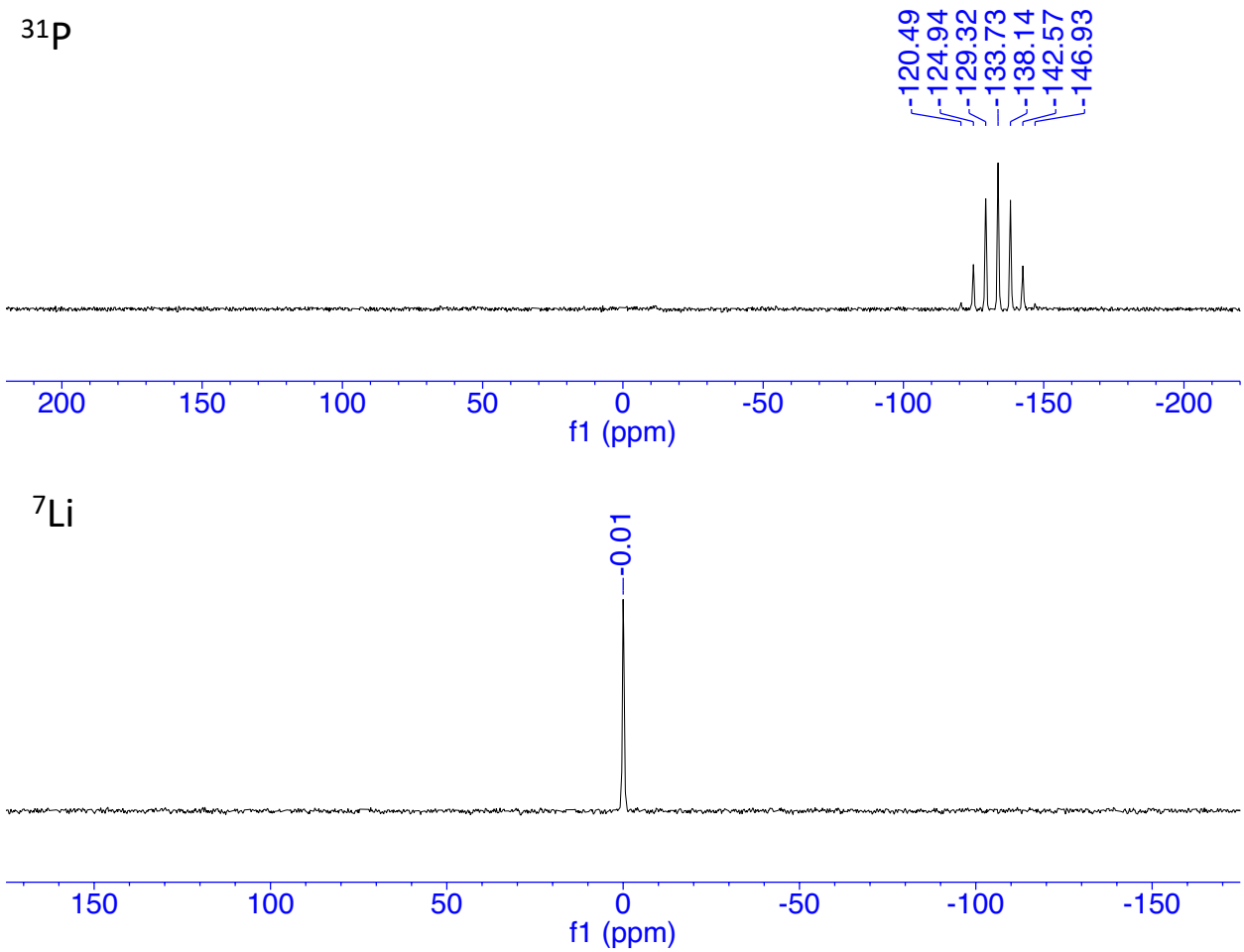

Figure S10. Solid state ^{31}P and ^{7}Li NMR spectra of **P2**•$LiPF_6$.

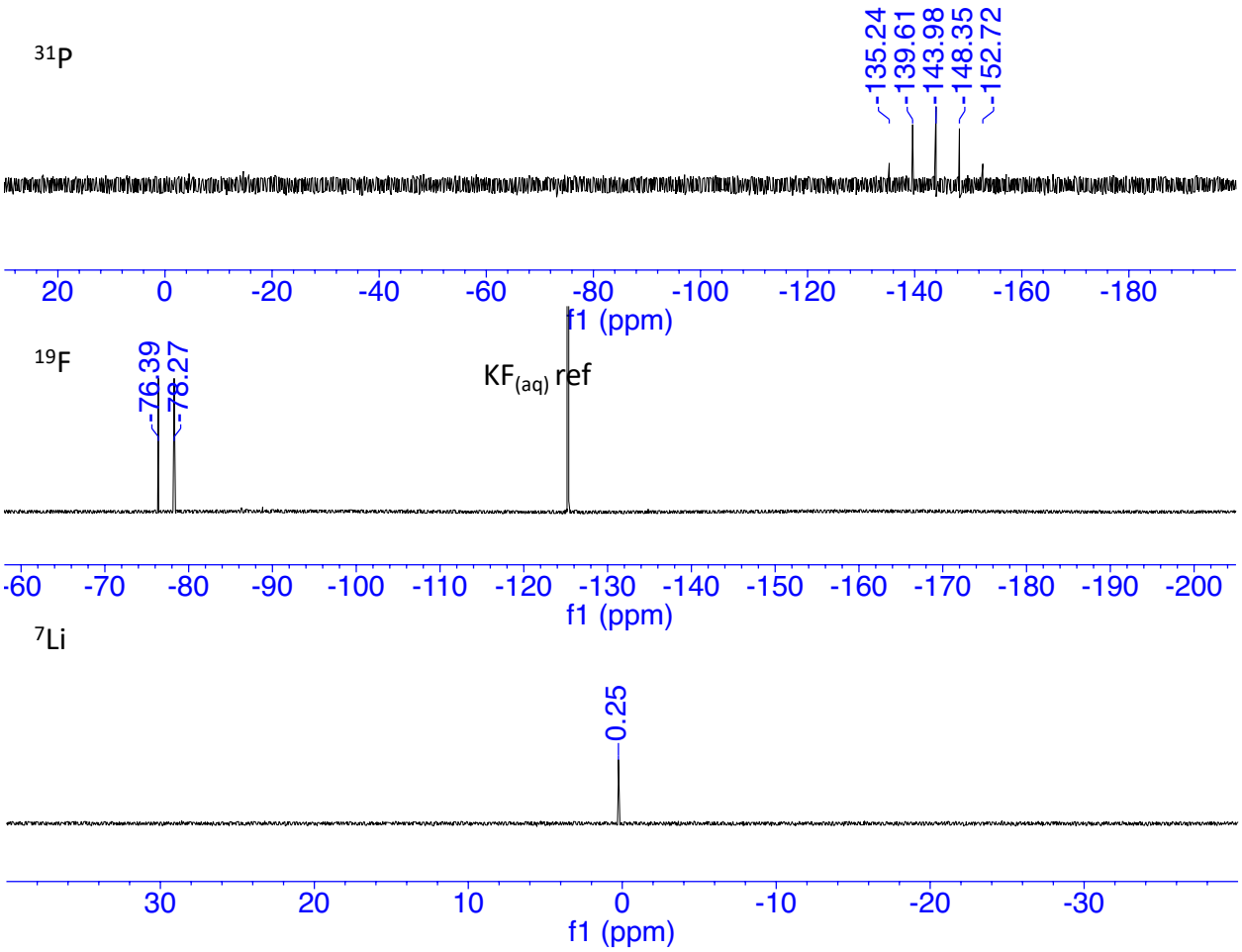

Figure S11. ^{31}P, ^{19}F, and ^{7}Li NMR spectra of the $LiPF_6$ presumed to be released in MeOH. A coaxial aqueous KF sample was used as an external reference for the ^{19}F NMR spectral studies.

Energy dispersive X-ray analysis of P2•$LiPF_6$

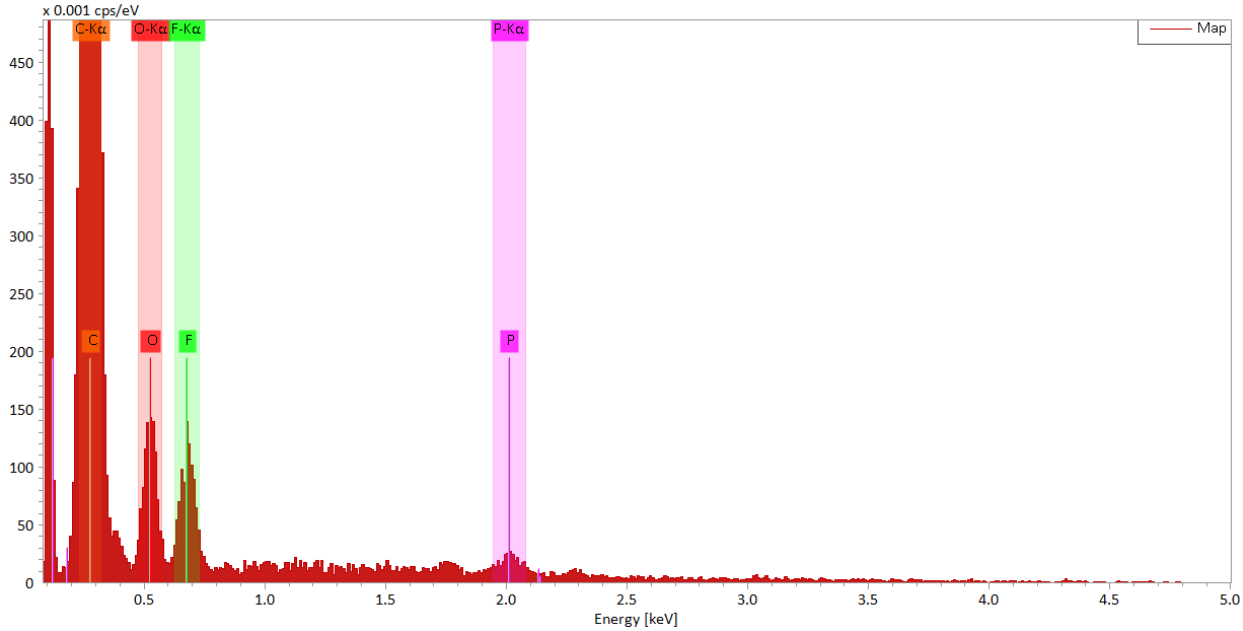

Figure S12. EDX spectrum of **P2**•$LiPF_6$.

Table S1. Elemental analysis of **P2**•$LiPF_6$ by EDX.

Element	Mass [%]	Mass Norm. [%]	Atom [%]
Carbon	79.29103	79.29103	85.2648381
Oxygen	9.6631873	9.6631873	7.80084737
Phosphorus	2.18786594	2.18786594	0.9123298
Fluorine	8.85791678	8.85791678	6.02198471
	100	100	100

Calibration curves for conductivity measurements of $LiPF_6$ concentration

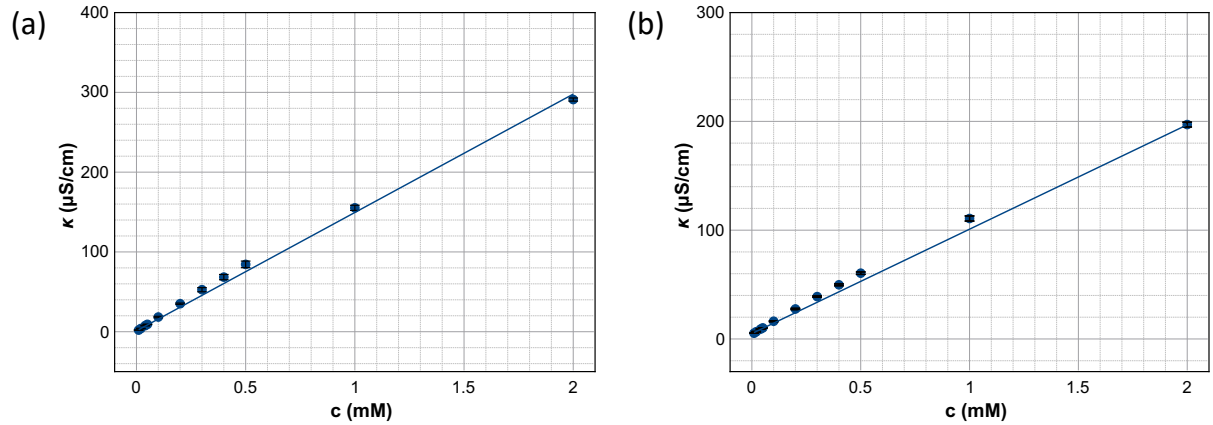

Figure S13. Calibration curves of $LiPF_6$ concentration determined by conductivity measurements in (a) acetonitrile and (b) MeOH. All solutions were prepared fresh and under N_2. Error bars represent s.d., n =3.

Fitting results:
ACN:
$R^2 = 0.9965$
$\kappa = 148.38\ c + 2.93$

MeOH:
$R^2 = 0.9913$
$\kappa = 95.96\ c + 2.85$

Quantitative NMR (qNMR) spectral studies

Acquisition time and the time delay were first optimized by acquiring the free induction decay (FID) spectrum and the T_1 relaxation times of the targeted species to ensure adequate collection of signals and thermal equilibrium. Battery grade lithium bis(trifluoromethanesulfonyl)imide (LITFSI) with purity 99.86% was used as a reference and as a standard in a coaxial setting.

A representative FID study of the ^{19}F nuclei in $LiPF_6$ revealed that most signal decays to noise level within 1.5 s (Figure S14).

T_1 relaxation times were determined by inversion recovery (INVREC) (Figure S15).

T_1 of ^{19}F of $LiPF_6$ in ACN =3.5 s

T_1 of ^{19}F of LiTFSI in D_2O = 4.2 s

Unless otherwise specified, these parameters were used for all quantitative ^{19}F NMR spectral studies.

Acquisition time = 1.5 s

Delay time (D1) = 30 s

The purity of samples was determined according to

$$P_s = \left(\frac{I_s}{I_R}\right)\left(\frac{V_R'}{V_S'}\right)\left(\frac{m_R}{m_S}\right)\left(\frac{MW_s}{MW_R}\right)\left(\frac{N_R}{N_S}\right)\left(\frac{V_S}{V_R}\right)P_R$$

where

P = purity

I = Integration

V' = the volume detected by NMR RF coil

m = mass

MW = molecular weight

N = number of the target nucleus

V = volume used dissolve the sample

S = sample

R = reference.

$\left(\frac{V_S'}{V_R'}\right) = 2.1144$ was determined according to a published procedure.[2]

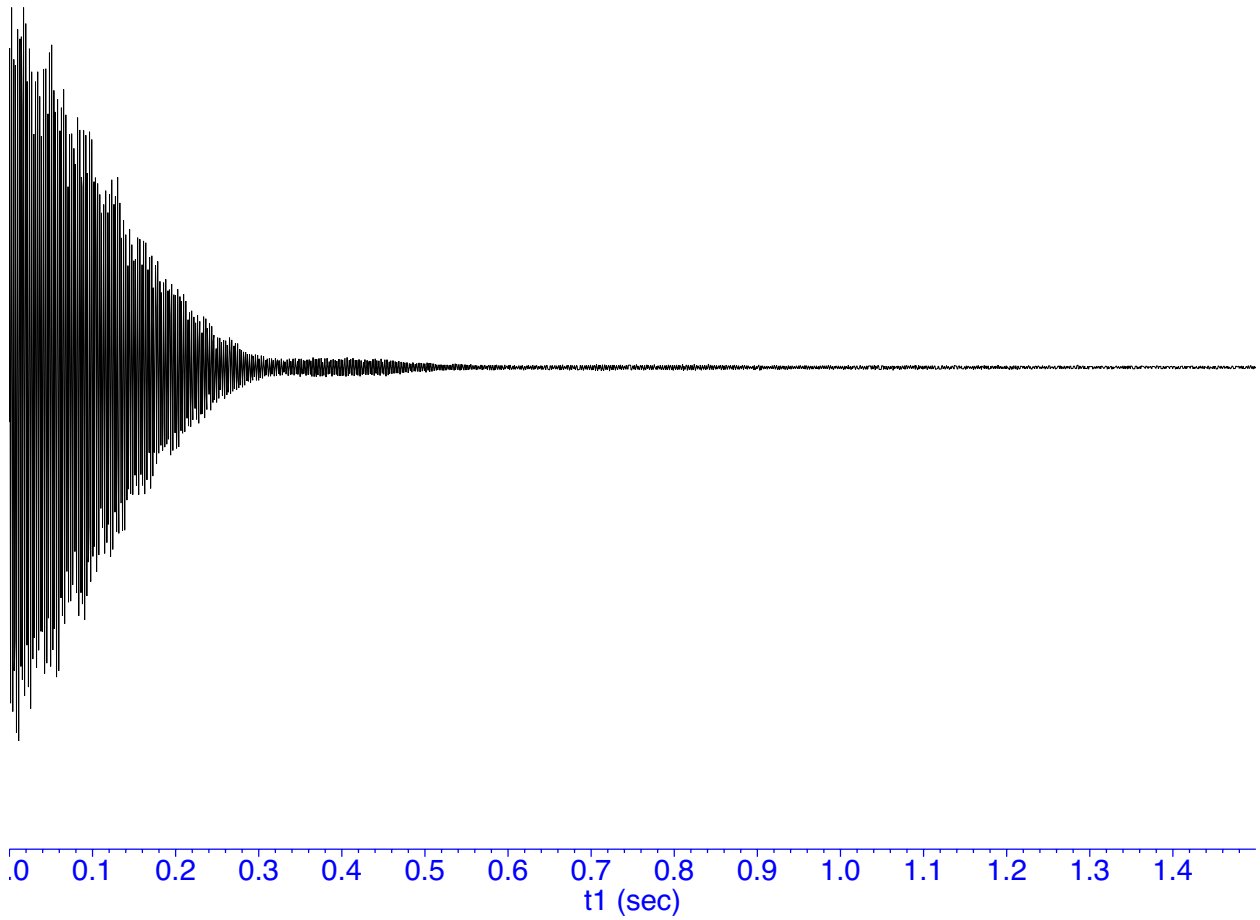

Figure S14. FID spectrum of ^{19}F in $LiPF_6$ as recorded in ACN.

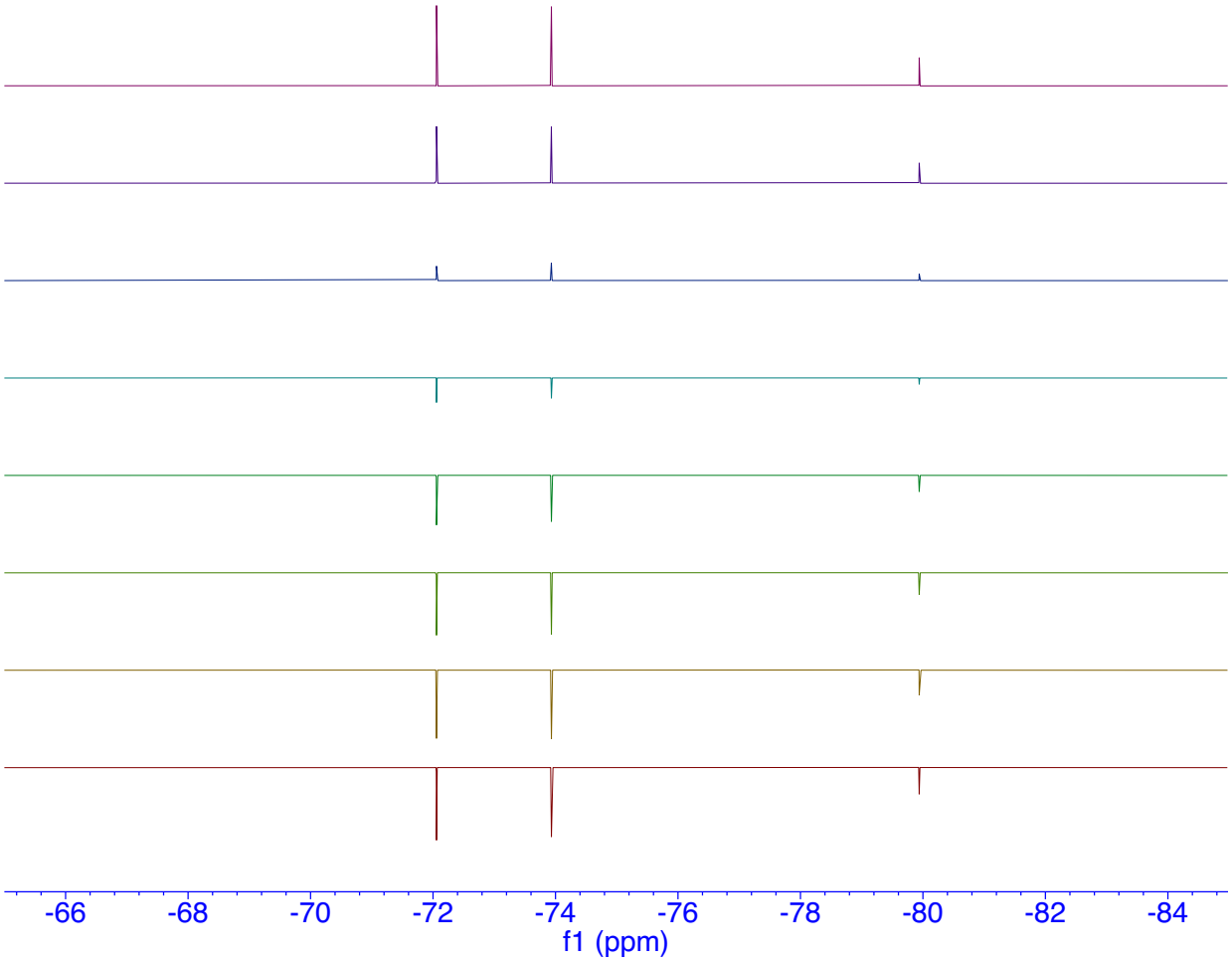

Figure S15. INVREC spectra of $LiPF_6$ in ACN. A coaxial sample of LiTFSI dissolved in D_2O was used as the reference at -80.26 ppm.

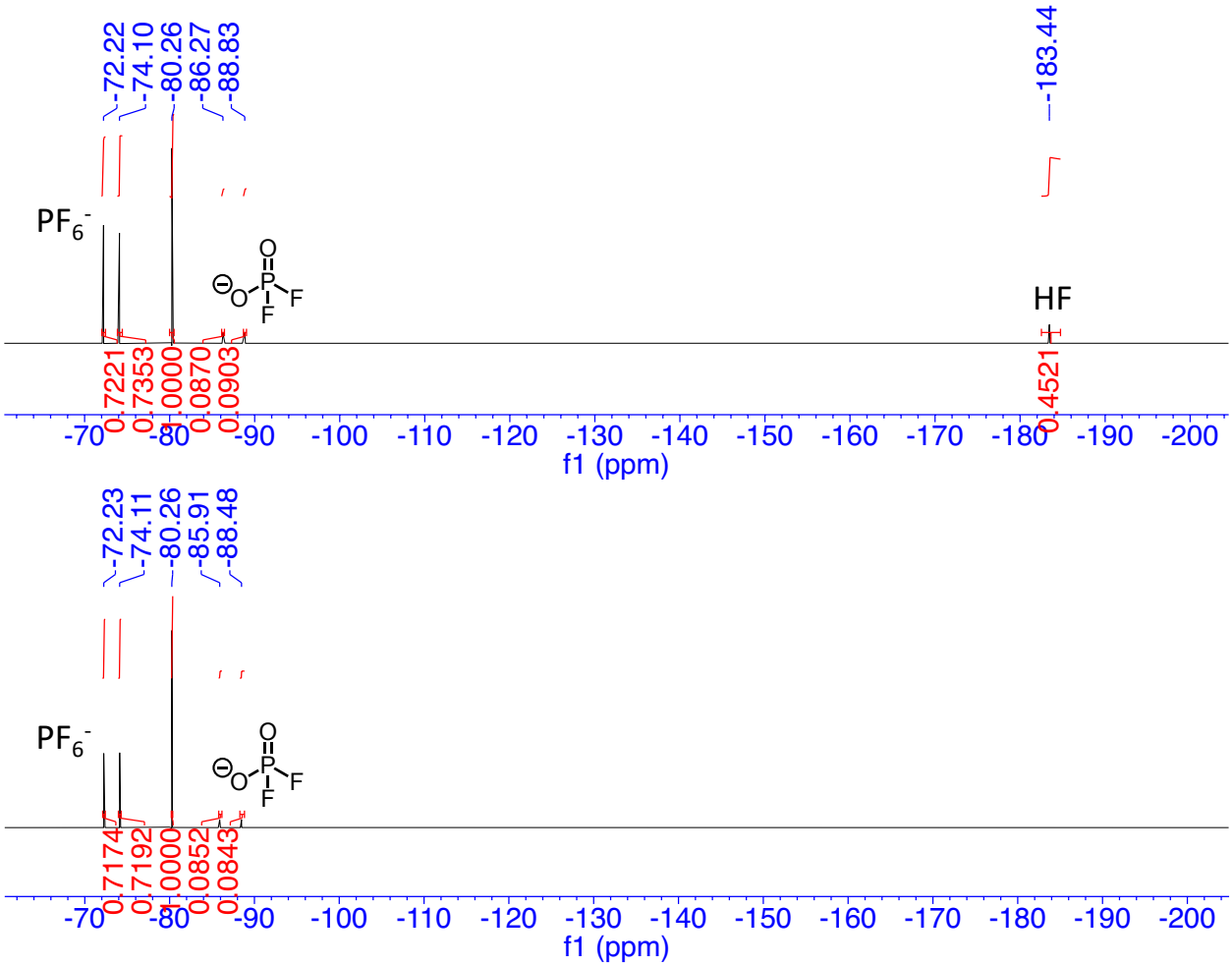

Figure S16. ^{19}F qNMR spectra of (a) degraded and (b) $K_2CO_{3(g)}$ neutralized samples. A coaxial sample of LiTFSI dissolved in D_2O was used as the reference at -80.26 ppm.

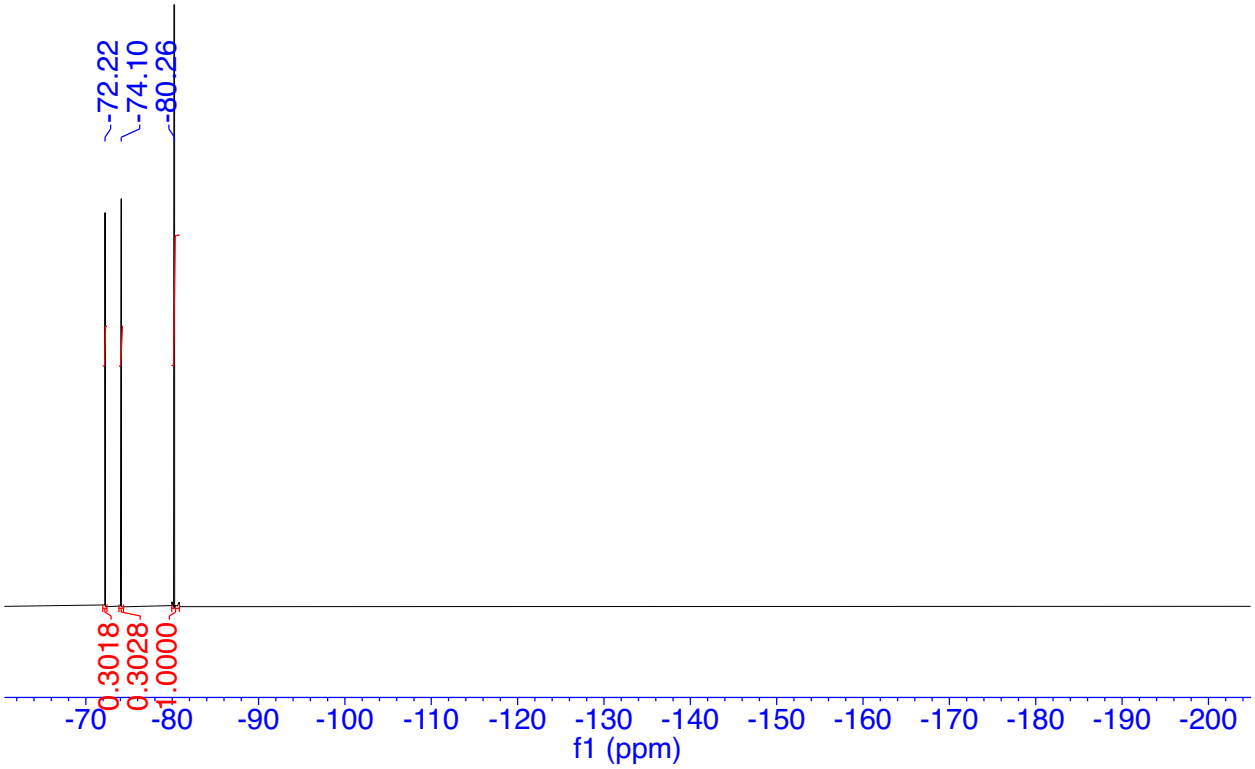

Figure S17. ^{19}F qNMR spectra of $LiPF_6$ in ACN. A coaxial sample of LiTFSI dissolved in D_2O was used as the reference at -80.26 ppm.

$$P_s = \left(\frac{I_s}{I_R}\right)\left(\frac{V_R'}{V_S'}\right)\left(\frac{m_R}{m_S}\right)\left(\frac{MW_s}{MW_R}\right)\left(\frac{N_R}{N_S}\right)\left(\frac{V_S}{V_R}\right)P_R$$

$$P_s = 0.6046 \times \left(\frac{1}{2.1144}\right) \times \left(\frac{14.2600}{2.8820}\right) \times \left(\frac{151.91}{287.08}\right) \times \left(\frac{6}{6}\right) \times \left(\frac{0.4}{0.3}\right) \times 99.86\% = 99.68\%$$

Table S2. ICP-MS result of the recovered product.

	Li	P	Al	Ca	Cd	Cr	Cu
Background (ppb)	-	2.72	27.58	69.28	-	0.07323	0.04638
Sample (ppb)	10.12	41.64	23.79	68.57	-	0.01601	0.02872
	Fe	K	Mg	Na	Ni	Pd	Zn
Background (ppb)	7.917	2.667	1.473	35.0	0.02295	0.06814	0.1591
Sample (ppb)	2.605	1.262	1.418	24.4	0.01041	0.06503	0.2253

NMR and MS spectra

Dima-BookI-Page18-1H-CDCl3-Re_PROTON_20220218_01

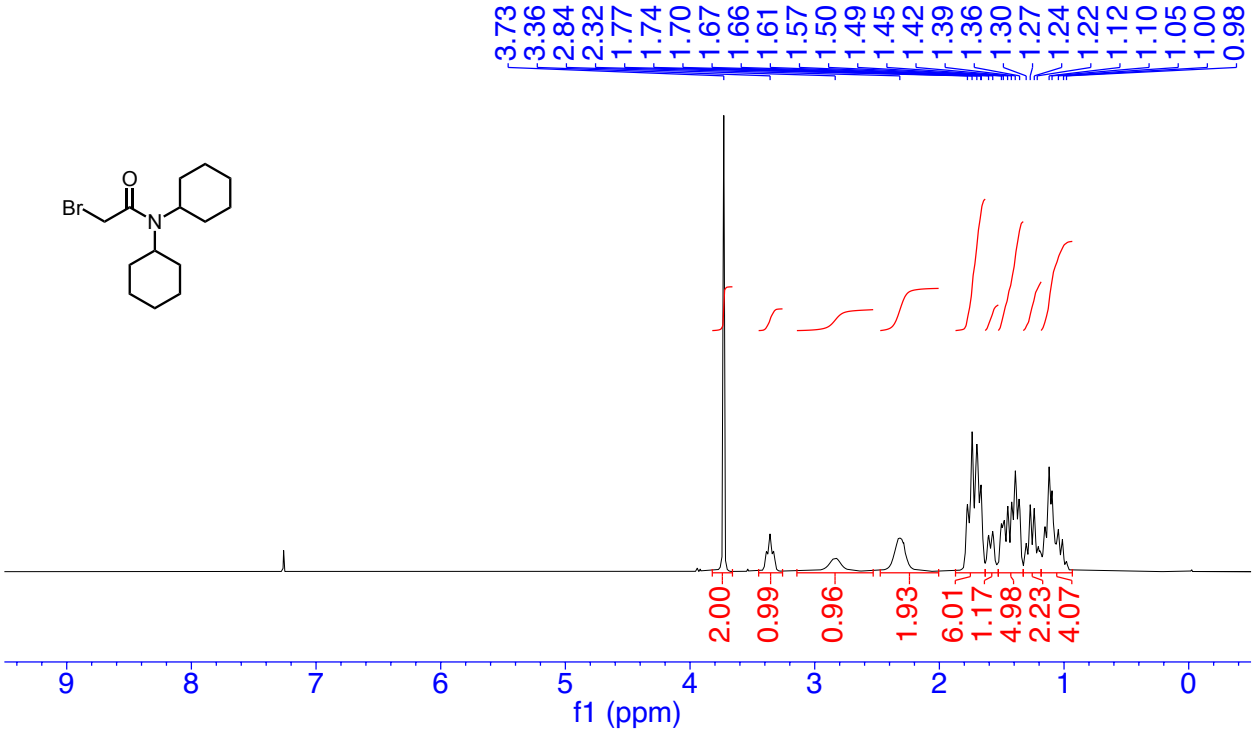

Figure S18. ^{1}H NMR spectrum of 2-bromo-*N,N*-dicyclohexylacetamide (400 MHz, $CDCl_3$).

Dima-BookI-Page18-13C-CDCl3-Re_CARBON_20220218_01

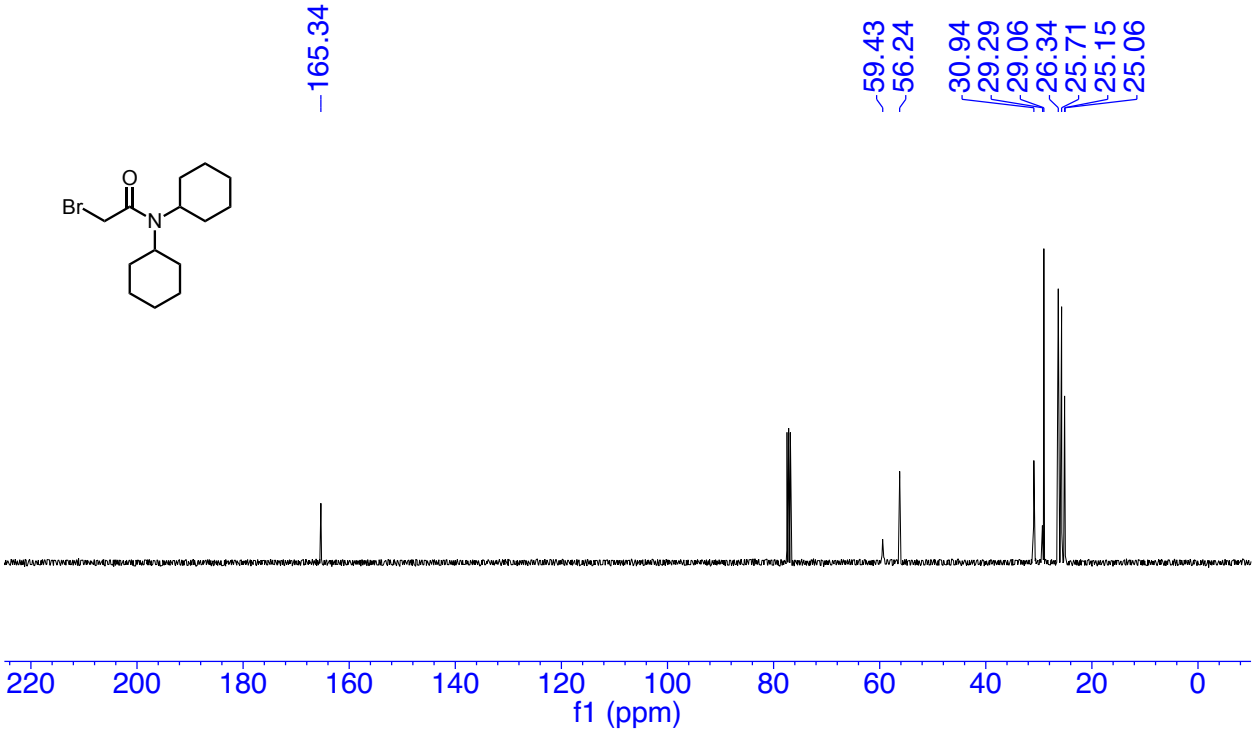

Figure S19. ^{13}C NMR spectrum of 2-bromo-*N,N*-dicyclohexylacetamide (100 MHz, $CDCl_3$).

Target Compound Screening Report

Results Acquired by The University of Texas at Austin Mass Spectrometry Facility

Data File	MSF22-0278(DCA)_hrESIpos1.d	**Sample Name**	0278(DCA)	**Comment**	0278(DCA)
Position	P1-D2	**Instrument Name**	Instrument 1	**User Name**	
Acq Method	FIA_pos.m	**Acquired Time**	2/18/2022 12:36:00 PM	**DA Method**	KS.m

MS Zoomed Spectrum

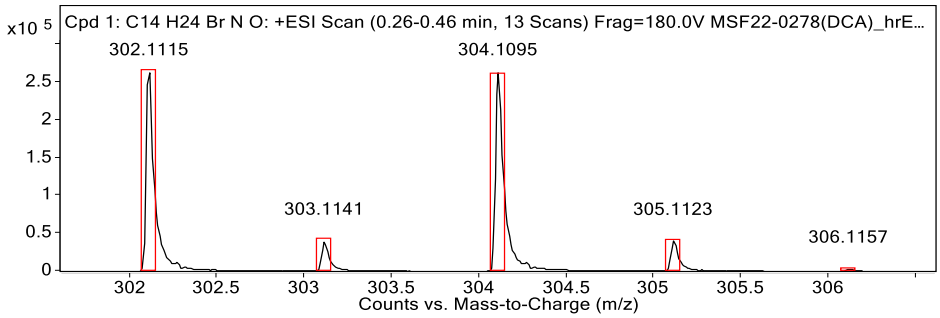

MS Spectrum Peak List

Obs. m/z	Calc. m/z	Charge	Abundance	Formula	Ion Species	Tgt Mass Error (ppm)
302.1115	302.1114	1	265344	C14H24BrNO	(M+H)+	-0.42
303.1141	303.1147	1	40433	C14H24BrNO	(M+H)+	1.89
304.1095	304.1095	1	263662	C14H24BrNO	(M+H)+	-0.2
305.1123	305.1127	1	40162	C14H24BrNO	(M+H)+	1.1
306.1157	306.1156	1	3439	C14H24BrNO	(M+H)+	-0.31
307.1392	307.1183	1	312	C14H24BrNO	(M+H)+	-68.16

--- End Of Report ---

Agilent Technologies Page 1 of 1 Printed at: 12:46 PM on:2/18/2022

Figure S20. ESI-HRMS spectrum of compound 2-bromo-N,N-dicyclohexylacetamide.

Dima-2022-1-20-BookI-Page90-2-1H-CDCl3_PROTON_20220120_01

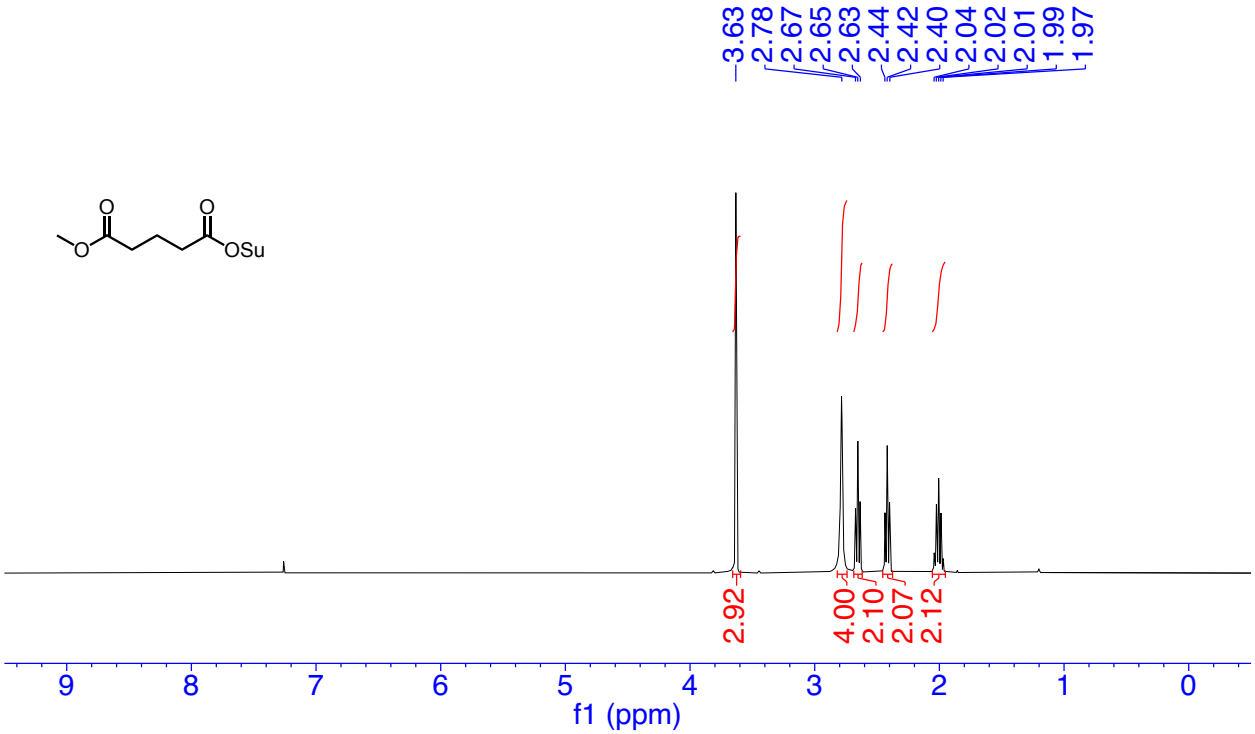

Figure S21. ^{1}H NMR spectrum of compound **1** (400 MHz, $CDCl_3$).

Dima-BookI-Page90-2-13C-CDCl3_CARBON_20220210_01

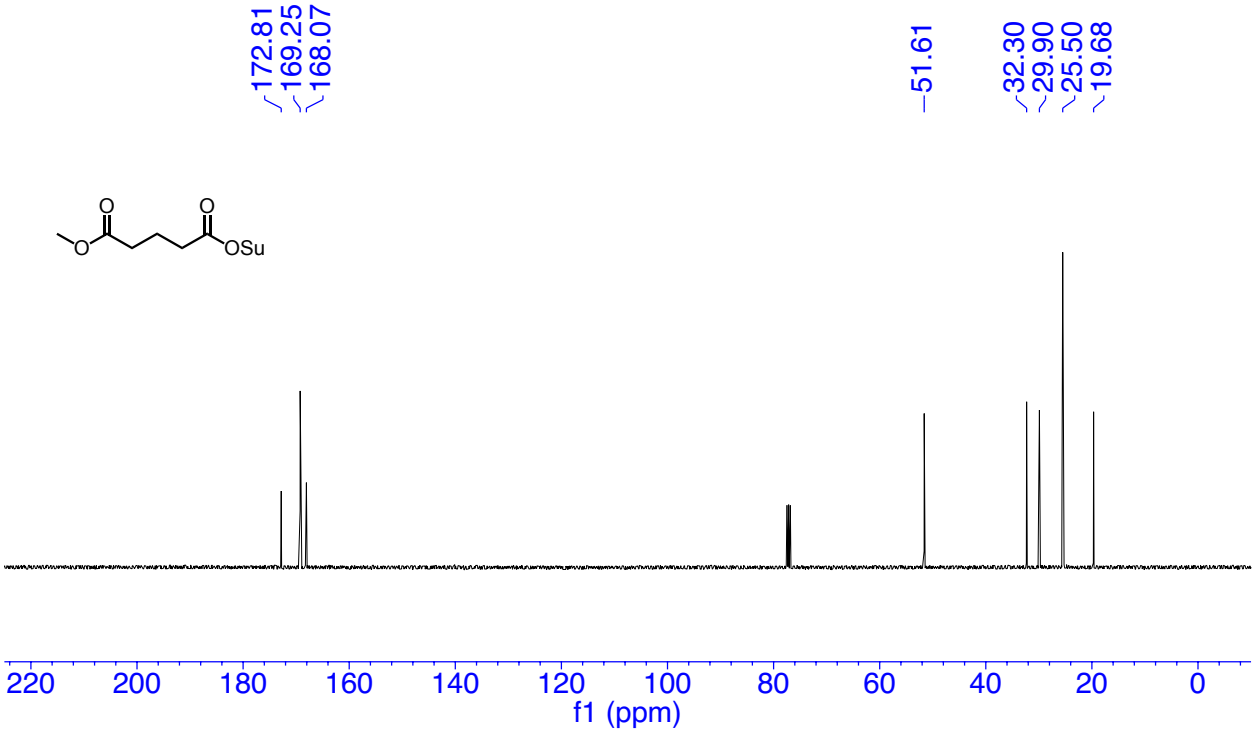

Figure S22. ^{13}C NMR spectrum of compound **1** (100 MHz, $CDCl_3$).

Target Compound Screening Report

Results Acquired by The University of Texas at Austin Mass Spectrometry Facility

Data File	MSF22-0277(Glutaric-OMe-OSu)_hrESIpos2.d	**Sample Name**	0277(Glutaric-OMe-OSu)	**Comment**	0277(Glutaric-OMe-OSu)
Position	P1-D1	**Instrument Name**	Instrument 1	**User Name**	
Acq Method	FIA_pos.m	**Acquired Time**	2/18/2022 12:47:17 PM	**DA Method**	KS.m

MS Zoomed Spectrum

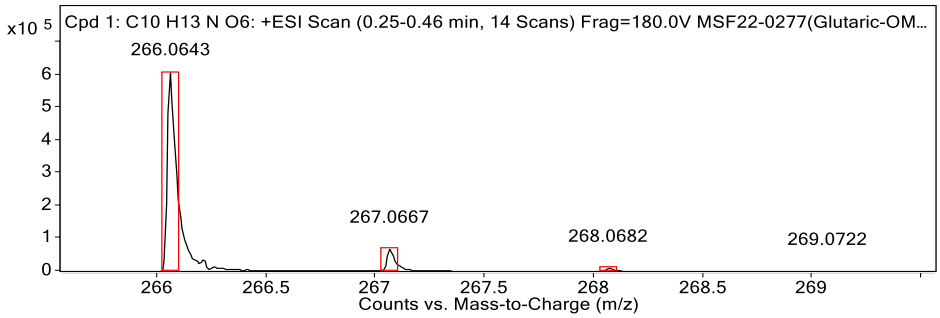

MS Spectrum Peak List

Obs. m/z	Calc. m/z	Charge	Abundance	Formula	Ion Species	Tgt Mass Error (ppm)
266.0643	266.0635	1	607394	C10H13NO6	(M+Na)+	-3.14
267.0667	267.0667	1	68725	C10H13NO6	(M+Na)+	0.09
268.0682	268.0685	1	10632	C10H13NO6	(M+Na)+	0.93
269.0722	269.0712	1	931	C10H13NO6	(M+Na)+	-3.75

--- End Of Report ---

Agilent Technologies Page 1 of 1 Printed at: 12:50 PM on:2/18/2022

Figure S23. ESI-HRMS spectrum of compound **1**.

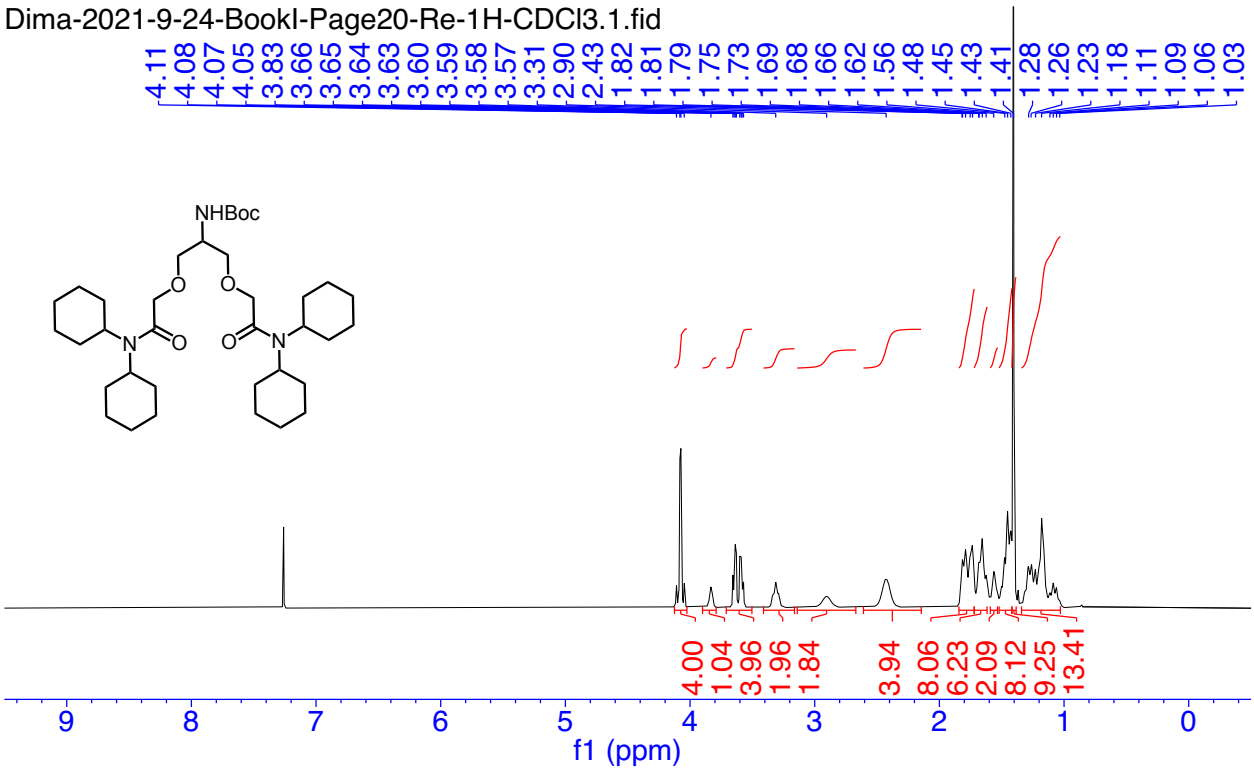

Figure S24. 1H NMR spectrum of compound **2** (400 MHz, $CDCl_3$).

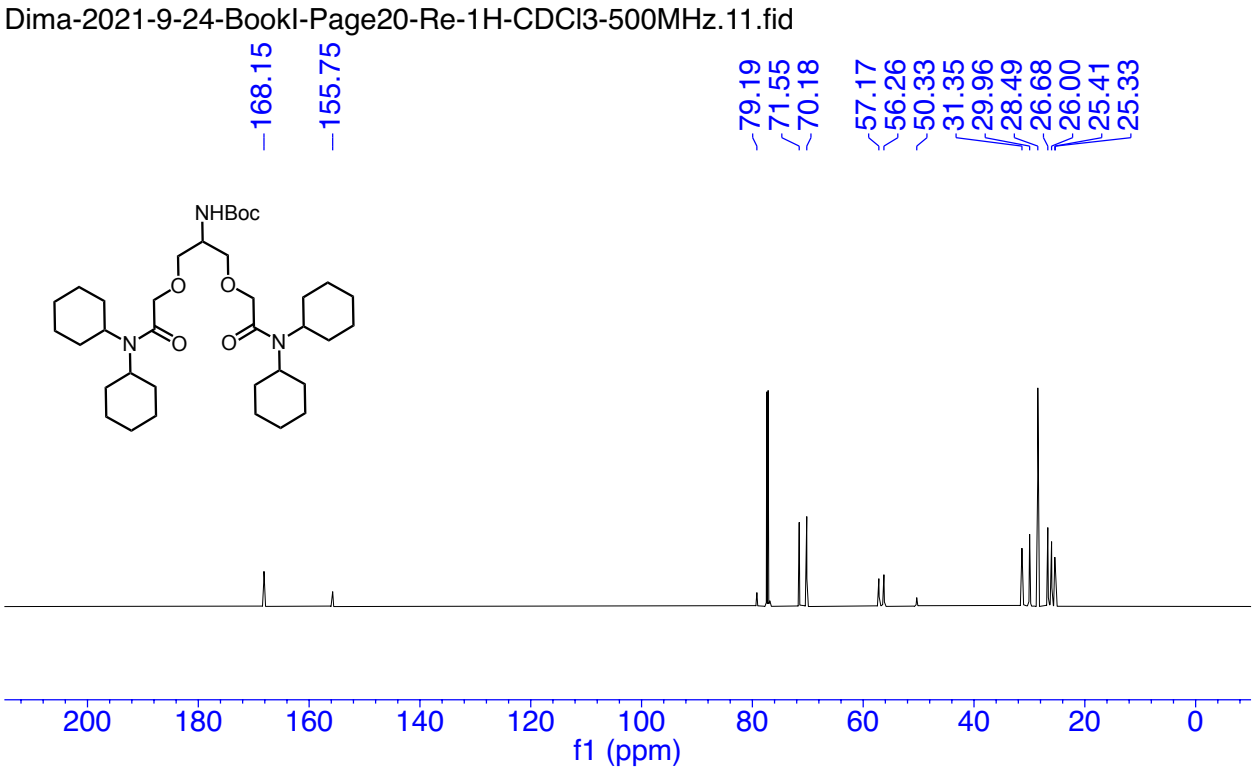

Figure S25. ^{13}C NMR spectrum of compound **2** (100 MHz, $CDCl_3$).

Target Compound Screening Report

Results Acquired by The University of Texas at Austin Mass Spectrometry Facility

Data File	MSF22-0279(Ser-Boc-DCA)_hrESIpos1.d	**Sample Name**	0279(Ser-Boc-DCA)	**Comment**	0279(Ser-Boc-DCA)
Position	P1-D3	**Instrument Name**	Instrument 1	**User Name**	
Acq Method	FIA_pos.m	**Acquired Time**	2/18/2022 12:37:37 PM	**DA Method**	KS.m

MS Zoomed Spectrum

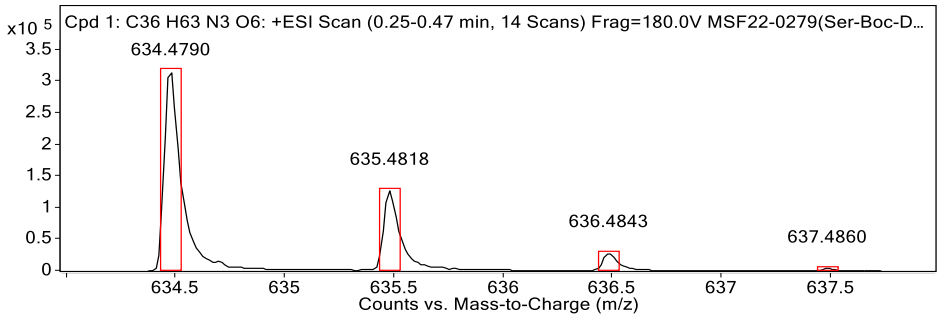

MS Spectrum Peak List

Obs. m/z	Calc. m/z	Charge	Abundance	Formula	Ion Species	Tgt Mass Error (ppm)
634.4790	634.4790	1	318746	C36H63N3O6	(M+H)+	0
635.4818	635.4822	1	127398	C36H63N3O6	(M+H)+	0.65
636.4843	636.4852	1	28772	C36H63N3O6	(M+H)+	1.42
637.4860	637.4880	1	4267	C36H63N3O6	(M+H)+	3.02
638.4894	638.4907	1	589	C36H63N3O6	(M+H)+	1.99

--- End Of Report ---

Agilent Technologies Page 1 of 1 Printed at: 1:29 PM on:2/18/2022

Figure S26. ESI-HRMS spectrum of compound **2**.

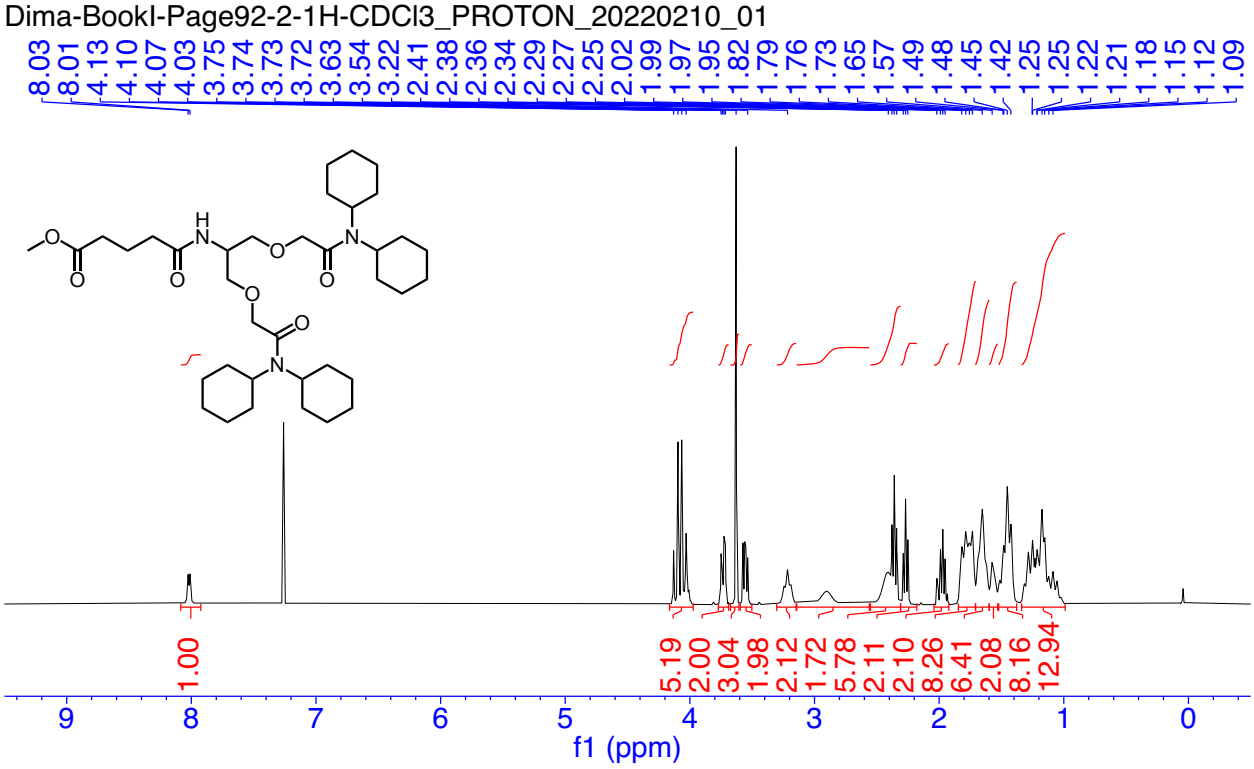

Figure S27. ^{1}H NMR spectrum of compound **3** (400 MHz, $CDCl_3$).

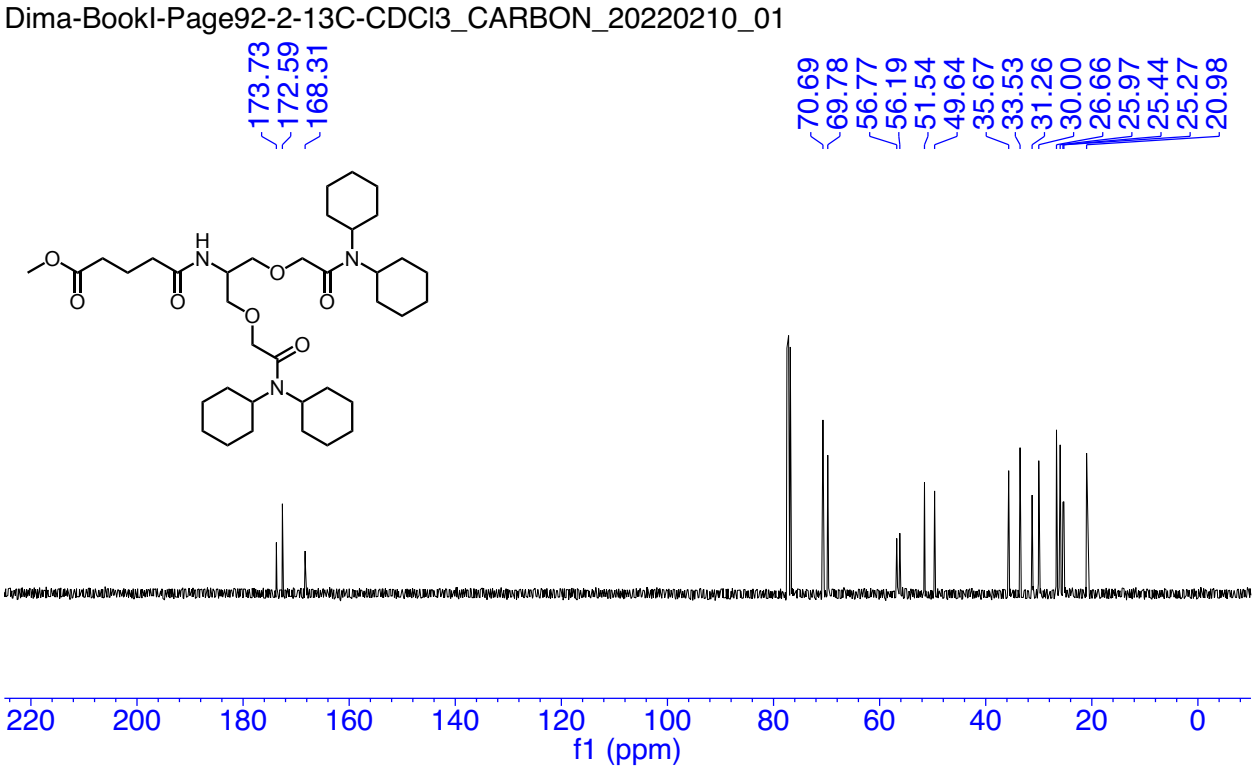

Figure S28. ^{13}C NMR spectrum of compound **3** (100 MHz, $CDCl_3$).

Target Compound Screening Report

Results Acquired by The University of Texas at Austin Mass Spectrometry Facility

Data File	MSF22-0280(Ser-Glutaric-DCA-OMe)_hrESIpos1.d	**Sample Name**	0280(Ser-Glutaric-DCA-OMe)	**Comment**	0280(Ser-Glutaric-DCA-OMe)
Position	P1-D4	**Instrument Name**	Instrument 1	**User Name**	
Acq Method	FIA_pos.m	**Acquired Time**	2/18/2022 12:39:18 PM	**DA Method**	KS.m

MS Zoomed Spectrum

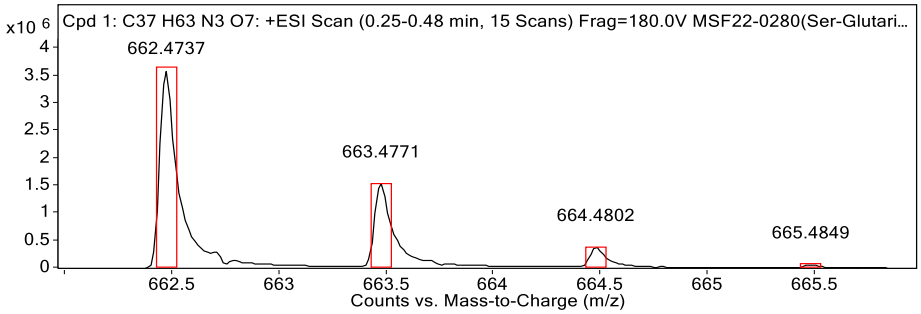

MS Spectrum Peak List

Obs. m/z	Calc. m/z	Charge	Abundance	Formula	Ion Species	Tgt Mass Error (ppm)
662.4737	662.4739	1	3595331	C37H63N3O7	(M+H)+	0.32
663.4771	663.4771	1	1545186	C37H63N3O7	(M+H)+	0.08
664.4802	664.4800	1	387699	C37H63N3O7	(M+H)+	-0.23
665.4849	665.4828	1	71595	C37H63N3O7	(M+H)+	-3.15
666.4870	666.4856	1	7519	C37H63N3O7	(M+H)+	-2.12

--- End Of Report ---

Agilent Technologies Page 1 of 1 Printed at: 1:33 PM on:2/18/2022

Figure S29. ESI-HRMS spectrum of compound **3**.

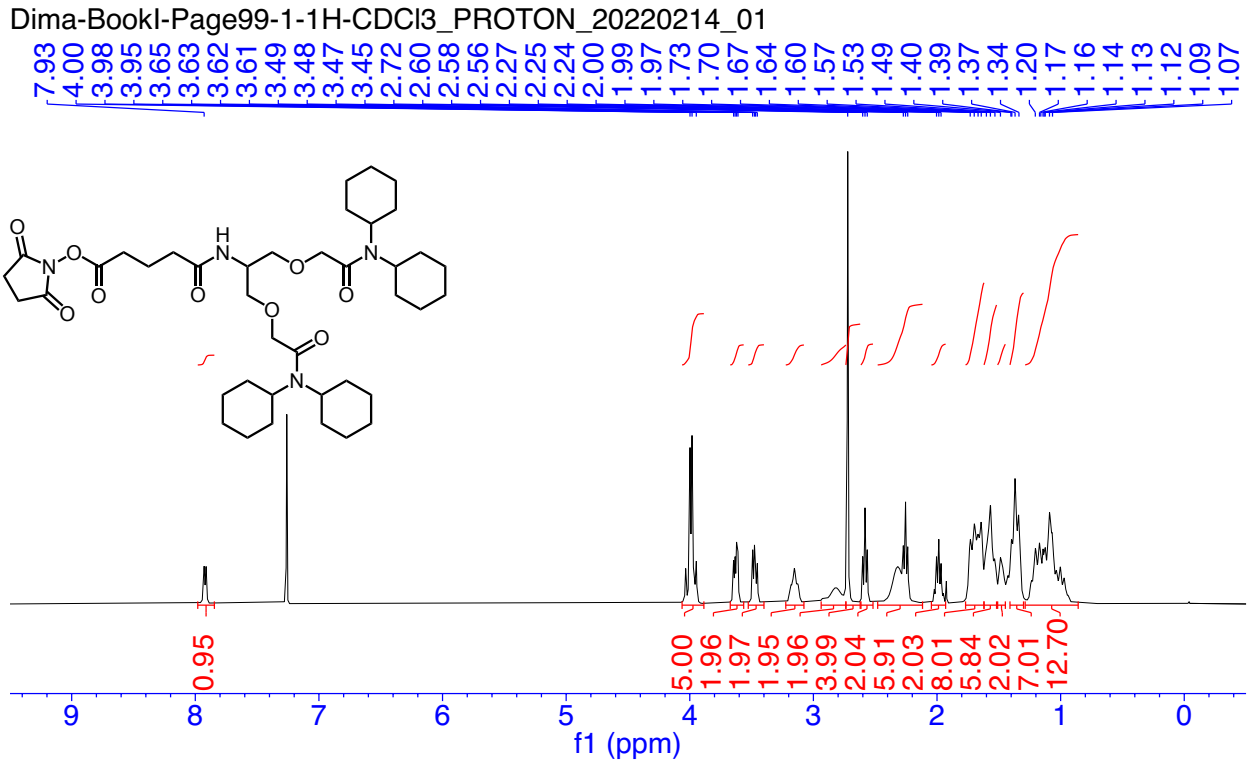

Figure S30. ^{1}H NMR spectrum of compound **4** (400 MHz, $CDCl_3$)

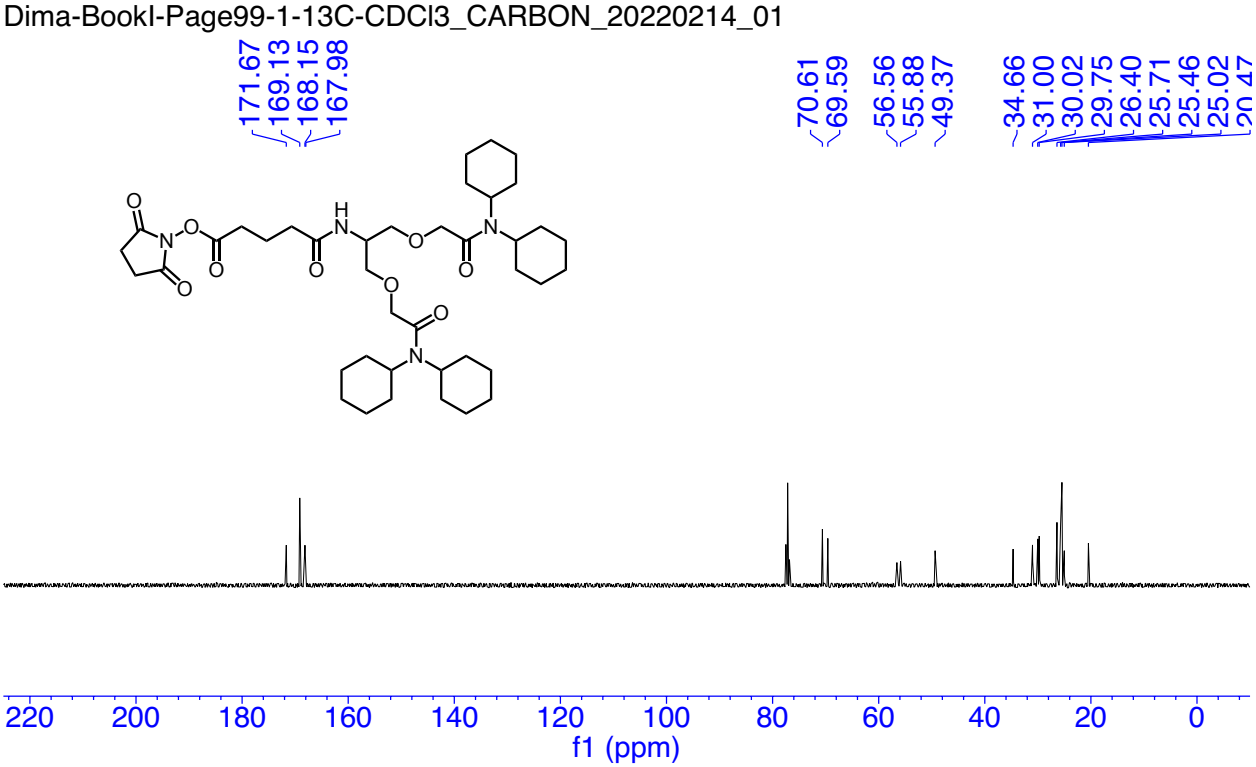

Figure S31. ^{13}C NMR spectrum of compound **4** (100 MHz, $CDCl_3$).

Target Compound Screening Report

Results Acquired by The University of Texas at Austin Mass Spectrometry Facility

Data File	MSF22-0276(Ser-Glutaric-DCA-OSu)_hrESIpos2.d	**Sample Name**	0276(Ser-Glutaric-DCA-OSu)	**Comment**	0276(Ser-Glutaric-DCA-OSu)
Position	P1-C9	**Instrument Name**	Instrument 1	**User Name**	
Acq Method	FIA_pos.m	**Acquired Time**	2/18/2022 12:44:57 PM	**DA Method**	KS.m

MS Zoomed Spectrum

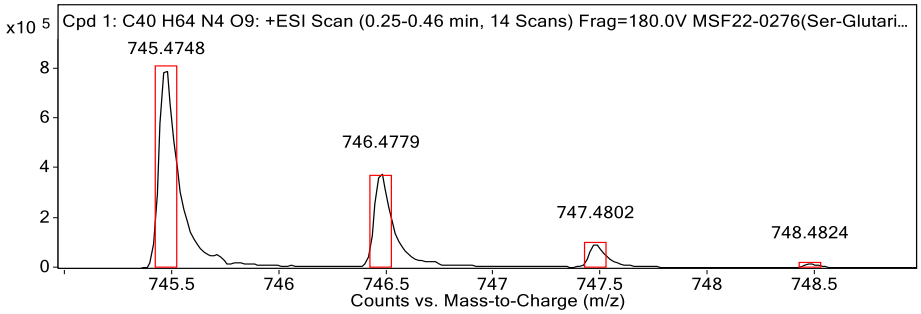

MS Spectrum Peak List

Obs. m/z	Calc. m/z	Charge	Abundance	Formula	Ion Species	Tgt Mass Error (ppm)
745.4748	745.4746	1	803459	C40H64N4O9	(M+H)+	-0.28
746.4779	746.4778	1	379617	C40H64N4O9	(M+H)+	-0.07
747.4802	747.4807	1	96903	C40H64N4O9	(M+H)+	0.65
748.4824	748.4834	1	15979	C40H64N4O9	(M+H)+	1.33
749.4874	749.4861	1	2499	C40H64N4O9	(M+H)+	-1.68
750.4979	750.4887	1	443	C40H64N4O9	(M+H)+	-12.14

--- End Of Report ---

Agilent Technologies Page 1 of 1 Printed at: 12:48 PM on:2/18/2022

Figure S32. ESI-HRMS spectrum of compound **4**.

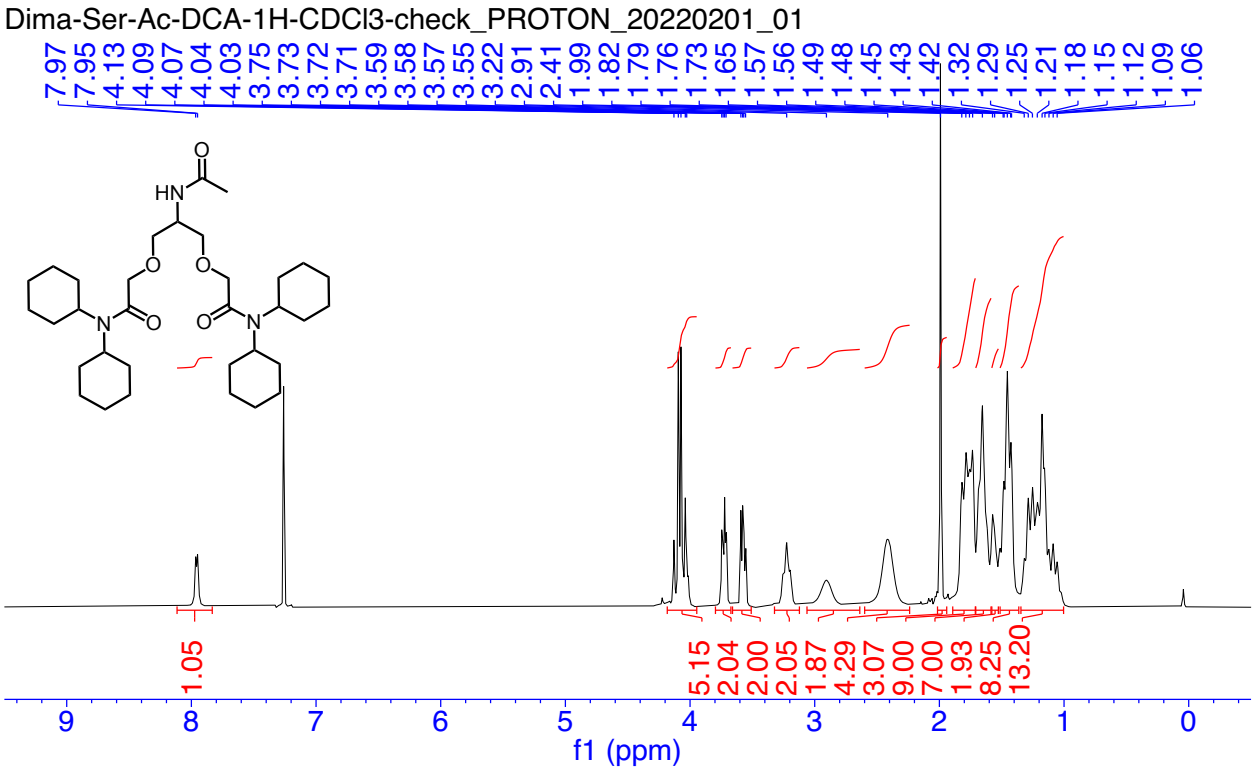

Figure S33. ^{1}H NMR spectrum of compound **L** (400 MHz, $CDCl_3$).

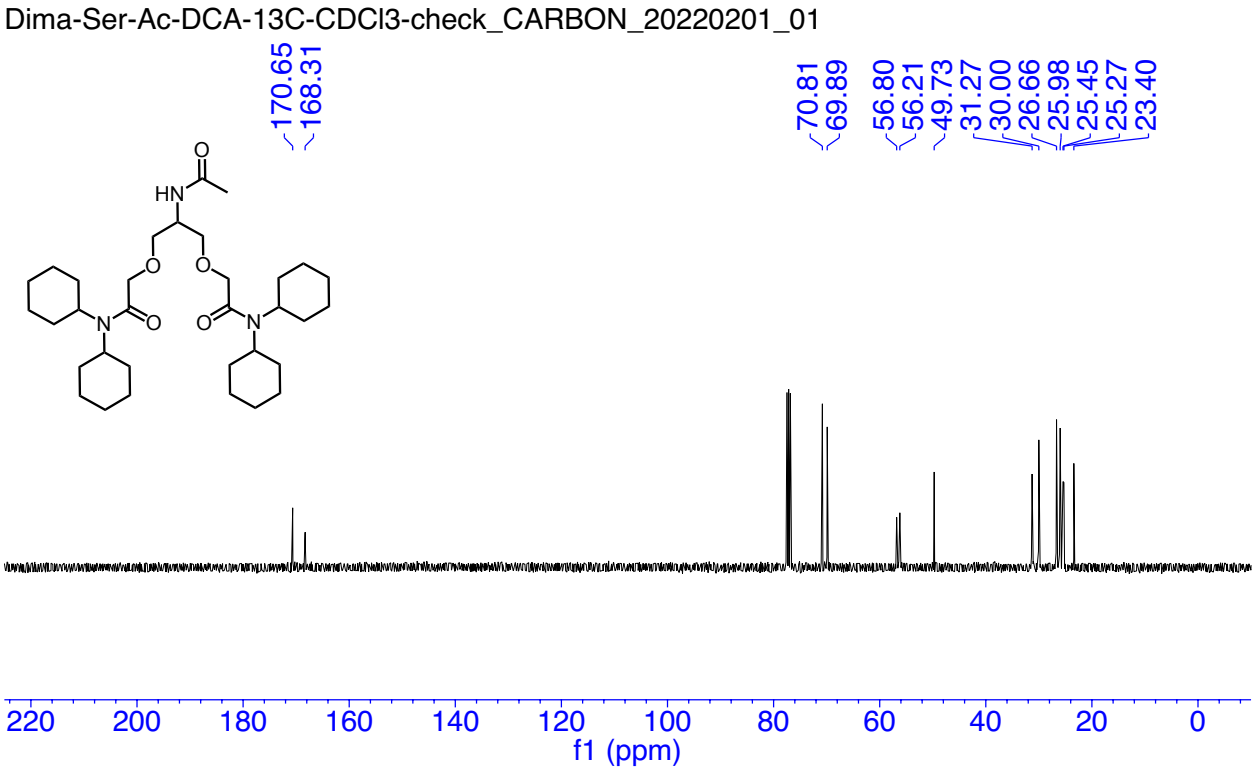

Figure S34. ^{13}C NMR spectrum of compound **L** (100 MHz, $CDCl_3$).

Target Compound Screening Report

Results Acquired by The University of Texas at Austin Mass Spectrometry Facility

Data File	MSF22-0274(Ser-Ac-DCA)_hrESIpos1.d	**Sample Name**	0274(Ser-Ac-DCA)	**Comment**	0274(Ser-Ac-DCA)
Position	P1-C7	**Instrument Name**	Instrument 1	**User Name**	
Acq Method	FIA_pos.m	**Acquired Time**	2/18/2022 12:29:20 PM	**DA Method**	KS.m

MS Zoomed Spectrum

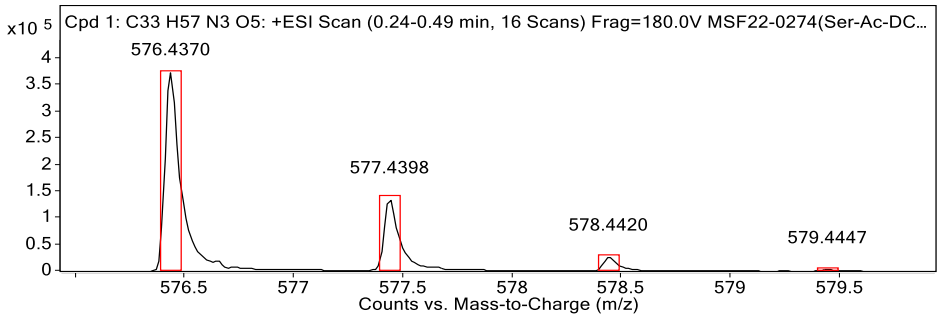

MS Spectrum Peak List

Obs. m/z	Calc. m/z	Charge	Abundance	Formula	Ion Species	Tgt Mass Error (ppm)
576.4370	576.4371	1	374447	C33H57N3O5	(M+H)+	0.13
577.4398	577.4403	1	135398	C33H57N3O5	(M+H)+	0.98
578.4420	578.4433	1	27628	C33H57N3O5	(M+H)+	2.16
579.4447	579.4461	1	3777	C33H57N3O5	(M+H)+	2.43
580.4471	580.4488	1	475	C33H57N3O5	(M+H)+	2.84

--- End Of Report ---

Agilent Technologies Page 1 of 1 Printed at: 12:41 PM on:2/18/2022

Figure S35. ESI-HRMS spectrum of compound **L**.

Cost Analyses

N-hydroxysuccinimide (NHS): 0.12/g (Oakwood chemicals)
EDCI: 0.28/g (Oakwood chemicals)
Trifluoroacetic acid (TFA): 0.088/g (Oakwood chemicals)
Note: The time for syntheses was not counted.

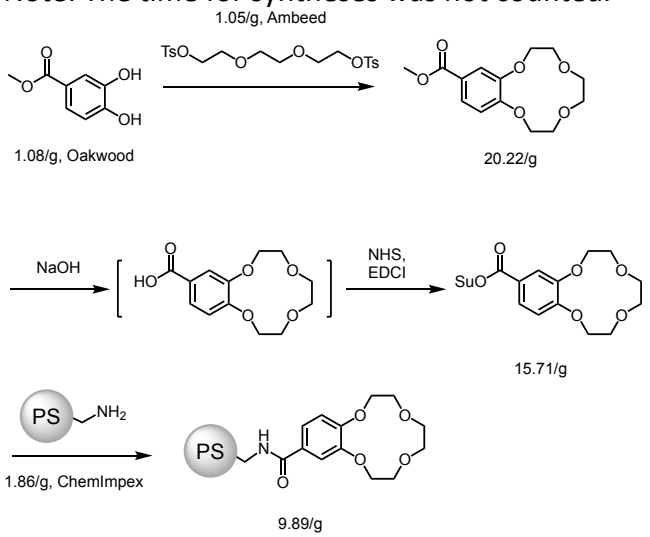

Figure S36. Cost analysis of crown-ether functionalized polystyrene resin.

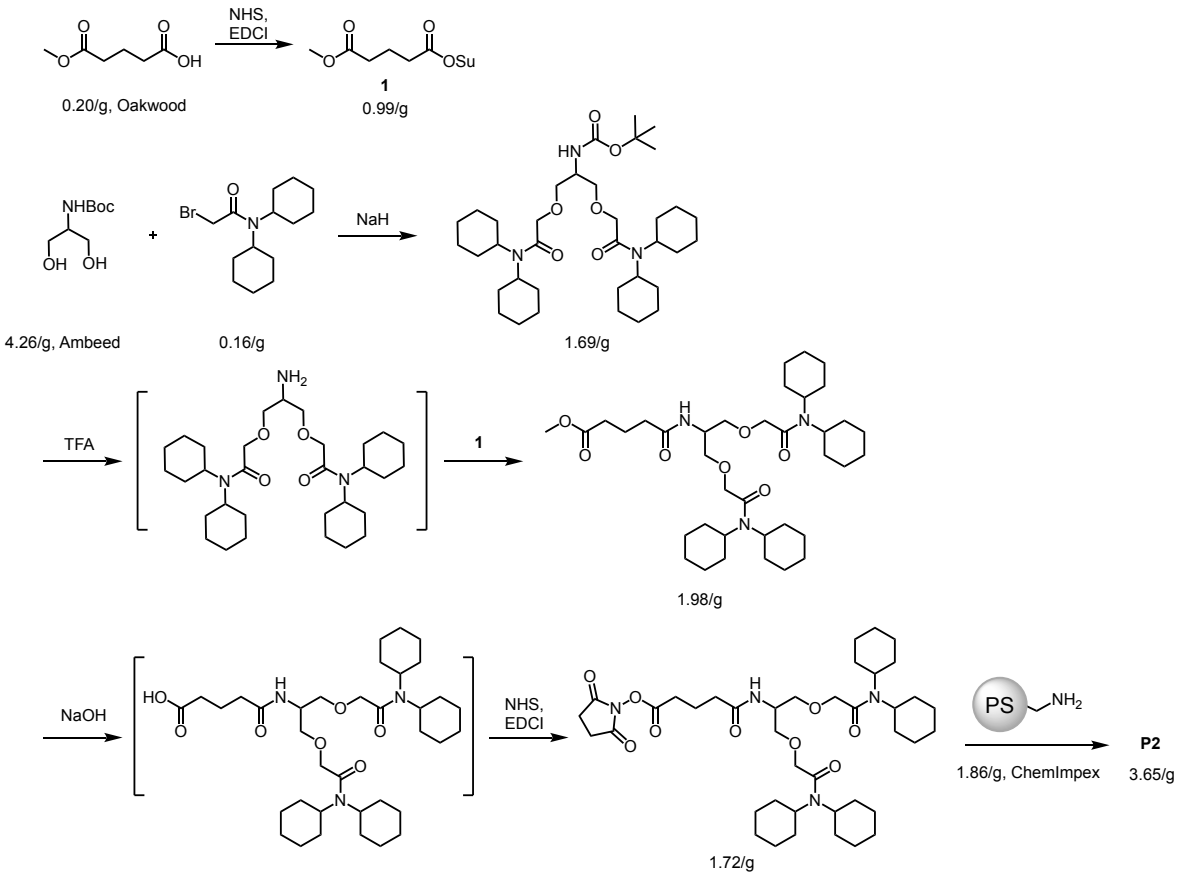

Figure S37. Cost analysis of **P2**.

X-Ray Photoelectron Spectroscopic Analyses

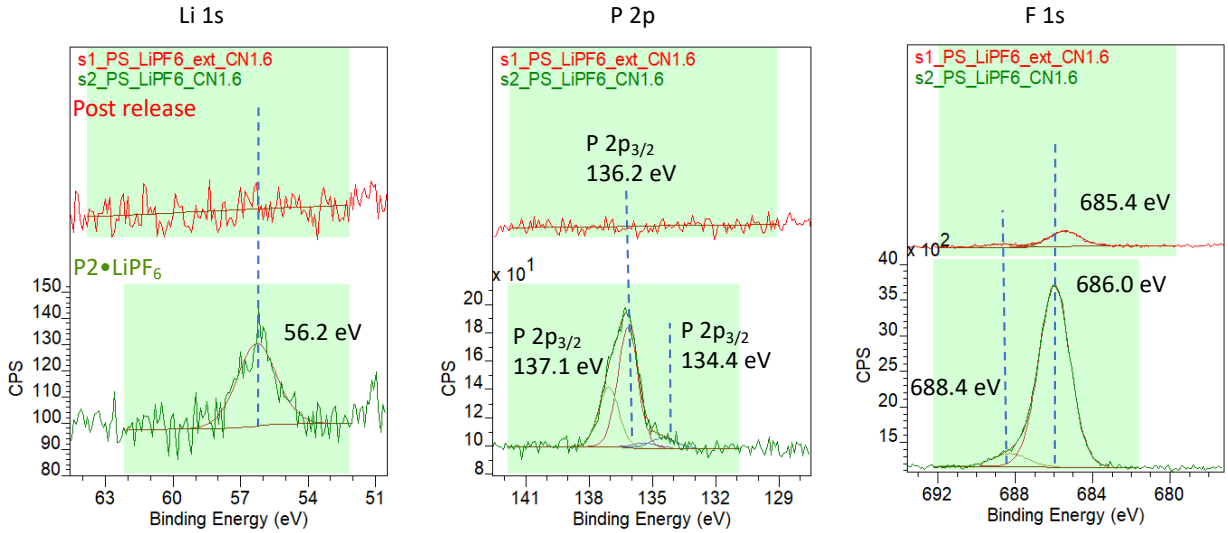

Figure S38. XPS analyses of **P2•**$LiPF_6$ (green) and **P2** (red).

References

1 F. Vögtle, T. Kleiner, R. Leppkes, M. W. Läubli, D. Ammann and W. Simon, *Chem. Ber.*, 1983, **116**, 2028–2034.

2 T. J. Henderson, *Anal. Chem.*, 2002, **74**, 191–198.